

Receive Combining vs. Multi-Stream Multiplexing in Downlink Systems with Multi-Antenna Users

Emil Björnson, *Member, IEEE*, Marios Kountouris, *Member, IEEE*, Mats Bengtsson, *Senior Member, IEEE*, and Björn Ottersten, *Fellow, IEEE*

Abstract—In downlink multi-antenna systems with many users, the multiplexing gain is strictly limited by the number of transmit antennas N and the use of these antennas. Assuming that the total number of receive antennas at the multi-antenna users is much larger than N , the optimal multiplexing gain can be achieved under many different receive strategies. For example, the abundance of receive antennas can be utilized to schedule users with near-orthogonal channels, for multi-stream multiplexing to users with well-conditioned channels, and/or to enable interference-aware receive combining. In this paper, we try to answer the question if the N data streams should be divided among few users (many streams per user) or many users (few streams per user, enabling receive combining). Analytical results are derived to show how user selection, spatial correlation, heterogeneous user conditions, and imperfect channel acquisition (quantization or estimation errors) affect the performance when sending the maximal number of streams or one stream per scheduled user—two extremes in stream allocation.

While contradicting observations on this topic have been reported in prior work, we show that selecting many users and allocating one stream per user (i.e., exploiting receive combining) is the best candidate under realistic conditions. This is explained by the provably stronger resilience towards spatial correlation and larger benefit from multi-user diversity. This fundamental result has positive implications for the design of downlink systems as it reduces the hardware requirements at the users.

Index Terms—Multi-user MIMO, channel estimation, quantized feedback, block-diagonalization, zero-forcing, receive combining.

I. INTRODUCTION

The performance of downlink wireless communication systems can be improved by multi-antenna techniques, which enable efficient utilization of spatial dimensions. Depending on the available channel state information (CSI), these dimensions can be used for enhanced reliability and/or spatial multiplexing of multiple data streams with controlled interference [1]. The downlink single-cell sum capacity (with perfect CSI) behaves as

$$\min(N, MK) \log_2(P) + \mathcal{O}(1) \quad (1)$$

The research leading to these results has received funding from the European Research Council under the European Community's Seventh Framework Programme (FP7/2007-2013) / ERC grant agreement number 228044. This work was presented in part at the IEEE Swedish Communication Technologies Workshop (Swe-CTW), Stockholm, October 2011.

E. Björnson, M. Bengtsson, and B. Ottersten are with the Signal Processing Laboratory, ACCESS Linnaeus Center, KTH Royal Institute of Technology, SE-100 44 Stockholm, Sweden (e-mail: emil.bjornson@ee.kth.se; mats.bengtsson@ee.kth.se; bjorn.ottersten@ee.kth.se). B. Ottersten is also with Interdisciplinary Centre for Security, Reliability and Trust (SnT), University of Luxembourg, L-1359 Luxembourg-Kirchberg, Luxembourg (email: bjorn.ottersten@uni.lu). M. Kountouris and E. Björnson is with SUPELEC (Ecole Supérieure d'Electricité), Gif-sur-Yvette, France (e-mail: marios.kountouris@supelec.fr).

where N is the number of base station antennas, K is the number of users, each user has M antennas ($M < N$), and P is the signal-to-noise ratio (SNR) defined as the total transmit power divided by the noise power. The number of users is typically large (i.e., $K \geq N$) and thus the optimal *multiplexing gain* is $\min(N, MK) = N$. The multiplexing gain will have a major impact on the throughput of future cellular networks, which are expected to increase the cell density and thereby achieve high SNRs in a power-efficient way [2].

The sum capacity in (1) can in theory be achieved using dirty-paper coding [3], but this non-linear scheme has impractical complexity and is very sensitive to CSI imperfections. Fortunately, the optimal multiplexing gain of N can be achieved by linear *spatial division multiple access* (SDMA) strategies [4], such as *block-diagonalization* (BD) [5], [6] and *zero-forcing with combining* (ZFC) [7], [8]. Such SDMA strategies transmit N simultaneous data streams, but can divide them among the users in different ways; the system can select between $\lceil \frac{N}{M} \rceil$ and N users to be active and allocate from 1 to M streams to each of them. This raises the fundamental design question of how the receive antennas at each user should be used to maximize the system performance. Inter-user interference degrades user performance, while the mutual interference between users' own streams can be handled by receive processing. Thus, it seems beneficial to only have a few active users and multiplex many streams to each of them, but one should keep in mind that every additional stream allocated to a user experiences a weaker channel gain than the previous streams. If fewer than M streams are allocated to a user, this user has degrees of freedom for interference-aware receive combining to achieve a strong effective channel and better spatial co-user compatibility. In other words, it is not clear whether receive antennas should be utilized for *multi-stream multiplexing* or *receive combining*, or perhaps something intermediate. The answer has a profound impact on wireless system design, including the CSI acquisition protocols and receiver architecture.

A. Related Work

The answer to the question above can, in principle, be obtained by studying which allocation of data streams and selection of linear precoding maximizes the sum-rate performance. Unfortunately, this optimization problem is nonconvex and combinatorial, thus only suboptimal strategies can be applied in practice. Such low-complexity algorithms have been proposed in [9]–[12], among others, by successively allocating

data streams to users in a greedy manner. Simulations in these papers indicate that fewer than N streams should be used when P and K are small, and that spatial correlation makes it beneficial to divide the streams among many users. Simulations in [10] indicates that the probability of allocating more than one stream per user is small when K grows large, but they only consider users with homogeneous channel conditions and all the referred papers assume perfect CSI.

The authors of [8] claim that transmitting at most one stream per user (i.e., exploiting receive combining) is desirable when there are many users in the system. They justify their statement using asymptotic results from [13], where this approach achieves the sum capacity as $K \rightarrow \infty$. But such argumentation ignores some important issues: 1) asymptotic optimality can also be proven with multiple streams per user;¹ 2) the performance at practical number of users is unknown (K needs to be very large to approach capacity); and 3) the analysis implies an unbounded asymptotic multi-user diversity gain, which is a modeling artifact of Rayleigh fading channels [15].

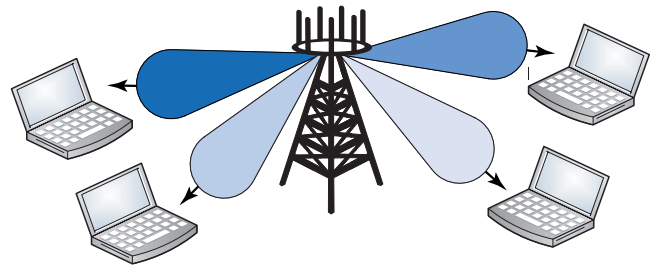
The authors of [6], [7] arrive at a different conclusion when they compare BD (which selects $\frac{N}{M}$ users and sends M streams/user) and ZFC (which selects N users and sends one stream/user) under quantized CSI. Their numerical analysis reveals a distinct advantage of BD (i.e., multi-stream multiplexing), but is limited to uncorrelated channels and neither includes user selection nor exploits interference rejection. Even under these suboptimal system conditions, we show herein that their results are misleading; their simulation considers a feedback load insufficient for SDMA, meaning that single-user transmission greatly outperforms both BD and ZFC.

B. Main Contributions

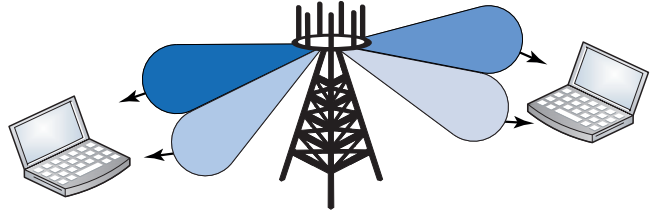
This paper provides a comprehensive answer to how multi-antenna users should utilize their antennas in downlink transmissions, or similarly how many data streams that should be allocated per active user under different system conditions; see Fig. 1. The main contributions are:

- New analytic results for analyzing the problem under spatial correlation, user selection, heterogeneous user channel conditions, and realistic CSI acquisition. These enable asymptotic comparison of the two extremes: allocating M streams per active user (asymptotically represented by BD) and one stream per active user (asymptotically represented by ZFC). We show that ZFC is more resilient to spatial correlation and well adapted to find near-orthogonal users, while BD is better at utilizing heterogeneous user conditions. Imperfect CSI acquisition is shown to have a similar impact on both strategies.
- Numerical illustrations show that allocating one stream per active user is essentially optimal under realistic system conditions, and we explain how other conclusions may arise. The main conclusion is therefore that utilizing

¹The uplink analysis in [14] shows that a non-zero (but bounded) number of users can use multiple streams, and the well-established uplink-downlink duality makes this result applicable also in our downlink scenario.

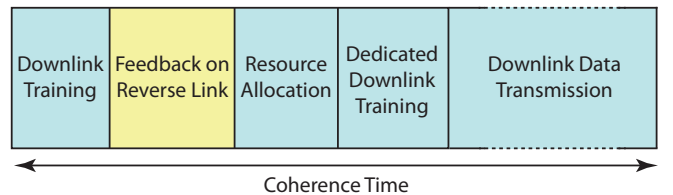


(a) 1 stream per 2-antenna user: ZFC enables receive combining.

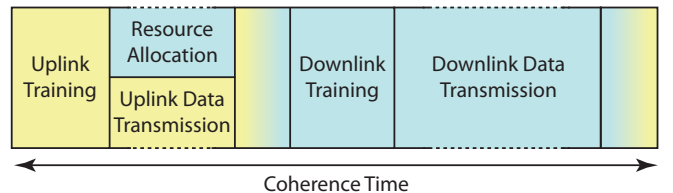


(b) 2 streams per 2-antenna user: BD exploits multi-stream multiplexing.

Fig. 1. Two ways of dividing four data streams among multi-antenna users, which also represents two ways of utilizing the receive antennas to reduce interference. (a) Receive one stream per user and linearly combine the antenna to achieve an effective channel that rejects interference. (b) Receive multiple streams and handle their mutual interference through receive processing.



(a) Basic cyclic operation of a block-fading FDD system.



(b) Basic cyclic operation of a block-fading TDD system.

Fig. 2. Basic system operation for FDD and TDD systems.

receive combining is preferable over multi-stream multiplexing.

II. SYSTEM MODEL

We consider a downlink multi-user MIMO system where a single base station with N antennas communicates with $K \geq N$ users. Each user has $M < N$ antennas and we will often assume that $\frac{N}{M}$ is an integer, for analytic convenience. The narrowband, flat-fading channel to user k is represented in the complex-baseband by $\mathbf{H}_k \in \mathbb{C}^{M \times N}$. The received signal at this user is

$$\mathbf{y}_k = \mathbf{H}_k \mathbf{x} + \mathbf{n}_k \quad (2)$$

where $\mathbf{x} \in \mathbb{C}^{N \times 1}$ is the transmitted signal and $\mathbf{n}_k \sim \mathcal{CN}(\mathbf{0}, \mathbf{I}_M)$ is the (normalized) noise vector. For analytic convenience and motivated by measurements [16], [17], we

employ the Kronecker model with $\mathbf{H}_k = \mathbf{R}_{R,k}^{1/2} \tilde{\mathbf{H}}_k \mathbf{R}_{T,k}^{1/2}$, where $\mathbf{R}_{T,k}$ and $\mathbf{R}_{R,k}$ are the positive-definite spatial correlation matrices at the transmitter and receiver side, respectively, and $\tilde{\mathbf{H}}_k$ has independent $\mathcal{CN}(0,1)$ -entries. We assume $\mathbf{R}_{T,k} = \mathbf{I}_N$ (i.e., large antenna separation at the base station) throughout the analysis, because transmit correlation both creates complicated mathematical structures and requires limiting assumptions on the user distribution geometry and fading environment. Observe that $\mathbf{R}_{R,k}$ generally is different for each users, describing different spatial properties.

To analyze the impact of imperfect CSI acquisition, we assume block fading where \mathbf{H}_k is static for a set of channel uses, called the *coherence time*, and then updated independently. We consider both frequency division duplex (FDD) and time division duplex (TDD); baselines of the respective cyclic system operations are illustrated in Fig. 2.

In FDD systems, users acquire CSI through training signaling [18] and some of the users feed back quantized CSI. The base station then performs resource allocation (i.e., stream allocation and precoding design) and informs the scheduled users of their precoding through a second training stage. Data transmission follows until the end of the coherence time, when the cycle in Fig. 2(a) restarts.

In TDD systems, the system toggles between uplink and downlink transmission on the same channel, which enables training signaling in both directions. We assume perfect channel reciprocity² and that the coherence time makes CSI obtained in one block of Fig. 2(b) reliable until we return to this block in the next cycle. The base station makes resource allocation decisions for both uplink and downlink, and it informs the users through training and control signaling.

We assume that all training signals sent in the downlink directions provide the users with perfect CSI, while CSI feedback (in FDD) and uplink training (in TDD) might lead to imperfect CSI at the base station. This assumption simplifies analysis as it enables coherent reception, thus making the achievable sum rate a reasonable measure.³ Observe that Fig. 2 only shows the main blocks of the system operations, while many types of control signaling are necessary in practice.

A. Linear Precoding: General Problem Formulation

We consider linear precoding and the transmitted signal is

$$\mathbf{x} = \sum_{k=1}^K \mathbf{W}_k \mathbf{d}_k \quad (3)$$

where $\mathbf{W}_k \in \mathbb{C}^{N \times d_k}$ is the precoding matrix, $\mathbf{d}_k \sim \mathcal{CN}(\mathbf{0}, \mathbf{I}_{d_k})$ is the data signal, and d_k is the number of multiplexed data streams to user k . If this user applies a semi-unitary receive combining matrix $\mathbf{C}_k \in \mathbb{C}^{M \times d_k}$ (i.e.,

²The physical channel is always reciprocal, but different transceiver hardware is typically used in the downlink and the uplink. Thus, careful calibration is necessary to utilize the reciprocity in practice.

³Many of the results herein can be extended to include imperfect CSI at the users in the resource allocation, followed by a second training stage that provides scheduled users with sufficiently accurate CSI of the precoded channels to enable coherent reception. See [19] for examples on this in FDD systems.

$\mathbf{C}_k^H \mathbf{C}_k = \mathbf{I}_{d_k}$) and treats inter-user interference as Gaussian noise, the achievable information rate becomes

$$g_k(\{\mathbf{W}_\ell\}, \mathbf{C}_k) = \log_2 \frac{\det\left(\mathbf{I}_{d_k} + \sum_{\ell=1}^K \mathbf{C}_k^H \mathbf{H}_k \mathbf{W}_\ell \mathbf{W}_\ell^H \mathbf{H}_k^H \mathbf{C}_k\right)}{\det\left(\mathbf{I}_{d_k} + \sum_{\ell \neq k} \mathbf{C}_k^H \mathbf{H}_k \mathbf{W}_\ell \mathbf{W}_\ell^H \mathbf{H}_k^H \mathbf{C}_k\right)} \quad (4)$$

where $\{\mathbf{W}_\ell\}$ denotes the set of all precoding matrices and ℓ is an arbitrary user index. The transmission is limited by an average power constraint of P , thus

$$\mathbb{E}\{\mathbf{x}^H \mathbf{x}\} = \sum_{k=1}^K \text{tr}\{\mathbf{W}_k \mathbf{W}_k^H\} \leq P. \quad (5)$$

Ideally, we would like to select the number of data streams d_k , the precoding matrices \mathbf{W}_k , and the receive combining matrices \mathbf{C}_k to maximize the sum rate,

$$\begin{aligned} & \underset{\{\mathbf{W}_k, \mathbf{C}_k, d_k\}}{\text{maximize}} && \sum_{k=1}^K g_k(\{\mathbf{W}_\ell\}, \mathbf{C}_k) \\ & \text{subject to} && \sum_{k=1}^K \text{tr}\{\mathbf{W}_k \mathbf{W}_k^H\} \leq P, \\ & && \mathbf{C}_k^H \mathbf{C}_k = \mathbf{I}_{d_k}, \quad d_k \geq 0 \quad \forall k. \end{aligned} \quad (6)$$

Unfortunately, this resource allocation problem is nonconvex and NP-hard (even for $N = 1$, see [20]), thus some simplifications are necessary to obtain practically feasible solutions. There are iterative algorithms that convergence to a stationary point of (6) (see [21] and references therein), but the cyclic system operation in this paper requires a non-iterative approach.

The ever-increasing demand for data traffic pushes toward dense cellular deployments that achieve high SNRs with retained power efficiency [2]. It is therefore of dominating importance to limit the inter-user interference, which we handle by including a constraint on zero interference between active users (implicitly requiring $\sum_{k=1}^K d_k \leq N$). Furthermore, we fix the receive combining matrix \mathbf{C}_k at some value $\tilde{\mathbf{C}}_k$, which makes sense from a CSI acquisition perspective as only the effective channel $\tilde{\mathbf{C}}_k^H \mathbf{H}_k$ needs to be obtained through feedback (in FDD) or training signaling (in TDD). As users are unaware of co-users, it is natural to let $\tilde{\mathbf{C}}_k$ contain the d_k strongest (left) singular vectors of \mathbf{H}_k —known as maximum ratio combining (MRC). Under imperfect CSI acquisition, $\tilde{\mathbf{C}}_k$ can instead be selected to improve the CSI accuracy [7], [8]. We now have a simplified resource allocation problem,

$$\begin{aligned} & \underset{\{\mathbf{W}_k, d_k\}}{\text{maximize}} && \sum_{k=1}^K \log_2 \det(\mathbf{I}_{d_k} + \tilde{\mathbf{C}}_k^H \mathbf{H}_k \mathbf{W}_k \mathbf{W}_k^H \mathbf{H}_k^H \tilde{\mathbf{C}}_k) \\ & \text{subject to} && \sum_{k=1}^K \text{tr}\{\mathbf{W}_k \mathbf{W}_k^H\} \leq P, \quad d_k \geq 0 \quad \forall k, \\ & && \tilde{\mathbf{C}}_k^H \mathbf{H}_k \mathbf{W}_\ell = \mathbf{0}_{d_k \times d_\ell} \quad \forall k, \forall \ell \neq k. \end{aligned} \quad (7)$$

When the precoding and stream allocation $\{\mathbf{W}_k^*, d_k^*\}$ have been determined for (7), the users are informed of the resource allocation through training and control signaling. This enables

estimation of both the precoded channel $\mathbf{H}_k \mathbf{W}_k$ and the second-order interference term $\mathcal{I}_k = \sum_{\ell \neq k} \mathbf{H}_k \mathbf{W}_\ell \mathbf{W}_\ell^H \mathbf{H}_k^H$, which are both necessary for coherent reception. As a nice by-product [8], this information enables user k to replace the preliminary receive combiner $\tilde{\mathbf{C}}_k$ with the rate-maximizing MMSE receive combiner $\mathbf{C}_k^{\text{MMSE}}$ that contains the left singular vectors of $(\mathbf{I}_M + \mathcal{I}_k)^{-1} \mathbf{H}_k \mathbf{W}_k$ [12]. This improves the information rate by relaxing the interference nulling into a balancing between signal gain and interference rejection. The analytic results will be derived using $\tilde{\mathbf{C}}_k$, while the MMSE receive combiner is used in simulations.

B. Linear Precoding: Two Extremes

For any feasible data stream allocation $\{d_k\}$, the sum rate maximizing precoding in (7) is achieved by classic SVD-based precoding (including water-filling for power allocation) [5]. The optimal solution to (7) can thus be obtained through exhaustive search over all possible stream allocations, but it quickly becomes infeasible as N and K increase. Fortunately, greedy algorithms for finding the scheduling set \mathcal{S} of users with $d_k > 0$ can perform remarkably close to optimum; see [9]–[12]. As greedy algorithms are hard to analyze mathematically, the analytic results in this paper compares two extremes in the stream allocation: *block-diagonalization (BD)* [5] and *zero-forcing with combining (ZFC)* [7], [8]. More flexible allocations are considered in the simulations.

Definition 1. (Block-Diagonalization Precoding) Let \mathcal{S}^{BD} be a scheduling set with at most $\frac{N}{M}$ users. For each user $k \in \mathcal{S}^{\text{BD}}$, we set $d_k = M$ and $\mathbf{W}_k = \mathbf{W}_k^{\text{BD}} \boldsymbol{\Upsilon}_k^{1/2}$, where \mathbf{W}_k^{BD} is a semi-unitary matrix that satisfies $\mathbf{W}_k^{\text{BD},H} \mathbf{W}_k^{\text{BD}} = \mathbf{I}_M$ and $\mathbf{H}_\ell \mathbf{W}_k^{\text{BD}} = \mathbf{0}$ for all $\ell \in \mathcal{S}^{\text{BD}} \setminus \{k\}$. The power allocation is given by the diagonal matrix $\boldsymbol{\Upsilon}_k \succeq \mathbf{0}_M$. The information rate is

$$g_k^{\text{BD}}(P) = \log_2 \det \left(\mathbf{I}_M + \mathbf{H}_k \mathbf{W}_k^{\text{BD}} \boldsymbol{\Upsilon}_k \mathbf{W}_k^{\text{BD},H} \mathbf{H}_k^H \right). \quad (8)$$

Definition 2. (Zero-Forcing Precoding with Combining) Each user combines its antennas using some channel-dependent unit-norm vector $\tilde{\mathbf{c}}_k \in \mathbb{C}^{M \times 1}$. Based on the effective channels $\mathbf{h}_k^H = \tilde{\mathbf{c}}_k^H \mathbf{H}_k \in \mathbb{C}^{1 \times N}$, a scheduling set \mathcal{S}^{ZFC} with at most N users is selected. For each user $k \in \mathcal{S}^{\text{ZFC}}$, we set $d_k = 1$ and let $\mathbf{W}_k = \sqrt{p_k} \mathbf{w}_k^{\text{ZFC}}$, where $\mathbf{w}_k^{\text{ZFC}}$ is a unit-norm vector that satisfies $\mathbf{h}_\ell^H \mathbf{w}_k^{\text{ZFC}} = 0$ for all $\ell \in \mathcal{S}^{\text{ZFC}} \setminus \{k\}$. The power $p_k \geq 0$ is allocated to user k and the information rate is

$$g_k^{\text{ZFC}}(P) = \log_2 \left(1 + p_k |\mathbf{h}_k^H \mathbf{w}_k^{\text{ZFC}}|^2 \right). \quad (9)$$

The sum-rate maximizing power allocations for BD and ZFC are achieved through water-filling (see [5]), but the asymptotic analysis in this paper often assumes equal power allocation (i.e., $\boldsymbol{\Upsilon}_k = \frac{P}{|\mathcal{S}^{\text{BD}}|} \mathbf{I}_M \forall k \in \mathcal{S}^{\text{BD}}$ and $p_k = \frac{P}{|\mathcal{S}^{\text{ZFC}}|} \forall k \in \mathcal{S}^{\text{ZFC}}$) since this becomes optimal in the high SNR regime ($P \rightarrow \infty$ [22]) where the system is interference-limited (and the effect of imperfect CSI is more pronounced)—this is practically relevant in dense cellular networks [2]. While the definitions of BD and ZFC assume perfect CSI, both strategies can be applied when the transmitter has imperfect CSI by pretending that the available CSI is perfect [6]–[8].

Both BD and ZFC precoding are designed to create zero inter-user interference, with the difference that ZFC only sends one data stream per scheduled user while BD selects fewer users but multiplexes M streams to each of them. BD and ZFC are identical when each user only has one antenna (i.e., $M = 1$). However, this does *not* mean that BD is a generalization of ZFC; there are good reasons for applying ZFC when $M > 1$:

- 1) The base station only needs to acquire the effective channels \mathbf{h}_k ;
- 2) The effective channels \mathbf{h}_k have better properties than \mathbf{H}_k and can be adapted for interference rejection;
- 3) User devices require simpler hardware that only decodes one stream.

The interference mitigation is, on the other hand, less restrictive under BD since fewer users are involved and the mutual interference between streams sent to the same user is handled by receive processing [6]. This paper compares the performance of ZFC and BD under both perfect and imperfect CSI. The results will provide an answer to the fundamental question of how to divide the available resources among multi-antenna users: should we select many users and enable receive combining or select few users and exploit multi-stream multiplexing?

Remark 1 (Ambiguous Terminology). The terminology *block-diagonalization* and *zero-forcing* have been given different meanings in prior work. Herein, BD refers to the original work in [5], where each active user receives exactly M data streams. Apart from the ZFC strategy in Definition 2 (and in [7], [8]), another downlink zero-forcing strategy for multi-antenna users was proposed in [23]. In their definition, each antenna at the multi-antenna users is viewed as a separate virtual single-antenna user and the zero-forcing idea is applied to send a separate stream to each antenna with zero inter-antenna interference. That approach is nothing else than BD with stricter interference mitigation and can *never* perform better than BD. Herein, ZFC means sending one stream per user and utilizing receive combining, thus ZFC is *not* a special case of BD and can hypothetically outperform BD.

III. COMPARISON OF BD AND ZFC WITH PERFECT CSI

In this section, we will compare BD and ZFC in the ideal scenario when both the base station and the users have perfect CSI. We derive analytic results showing the impact of different system properties. Under perfect CSI, the achievable sum rate in (7) asymptotically becomes (as $P \rightarrow \infty$) [22]

$$\begin{aligned} f_{\text{sum}}^{\text{BD}}(P) &\cong N \log_2 \left(\frac{P}{N} \right) + \sum_{k \in \mathcal{S}^{\text{BD}}} \log_2 \det \left(\mathbf{H}_k \mathbf{W}_k^{\text{BD}} \mathbf{W}_k^{\text{BD},H} \mathbf{H}_k^H \right), \\ f_{\text{sum}}^{\text{ZFC}}(P) &\cong N \log_2 \left(\frac{P}{N} \right) + \sum_{k \in \mathcal{S}^{\text{ZFC}}} \log_2 \left(|\mathbf{h}_k^H \mathbf{w}_k^{\text{ZFC}}|^2 \right), \end{aligned} \quad (10)$$

for BD and ZFC, respectively. This result is based on having scheduling sets that satisfy $|\mathcal{S}^{\text{BD}}| = \frac{N}{M}$ and $|\mathcal{S}^{\text{ZFC}}| = N$ and on equal power allocation (which is asymptotically optimal).

For both strategies, the asymptotic sum rate behaves as $\mathcal{M}_\infty \log_2(P) + \mathcal{R}_\infty$, where \mathcal{M}_∞ is the multiplexing gain

and \mathcal{R}_∞ is the rate offset. Both BD and ZFC achieve a multiplexing gain of $\mathcal{M}_\infty = N$, which is the same high-SNR slope as of the sum capacity. We thus need to compare the rate offsets \mathcal{R}_∞ to conclude which strategy is preferable.

Theorem 1. Assume that the receive correlation matrices $\mathbf{R}_{R,k}$ have eigenvalues $\lambda_{k,M} \geq \dots \geq \lambda_{k,1} > 0$ and random user selection with $|\mathcal{S}^{\text{BD}}| = \frac{N}{M}$, $|\mathcal{S}^{\text{ZFC}}| = N$. The expected asymptotic difference in sum rate between BD and ZFC is

$$\begin{aligned} \bar{\beta}_{\text{BD-ZFC}} &= \lim_{P \rightarrow \infty} \mathbb{E}\{f^{\text{BD}}(P) - f^{\text{ZFC}}(P)\} \\ &\leq N \frac{\log_2(e)}{M} \sum_{i=1}^{M-1} \frac{M-i}{i} + \log_2 \left(\frac{\prod_{k \in \mathcal{S}^{\text{BD}}} \prod_{m=1}^M \lambda_{k,m}}{\prod_{\ell \in \mathcal{S}^{\text{ZFC}}} \lambda_{\ell,M}} \right). \end{aligned} \quad (11)$$

Proof: The proof is given in Appendix B. ■

The expected asymptotic difference in Theorem 1 consists of two terms. The first term is positive and is an upper bound on the expected gain of BD in an uncorrelated system with homogenous users (cf. [22, Theorem 3]). The second term contains a ratio of eigenvalues, belonging to different users.

For users with homogenous channel conditions where all $\mathbf{R}_{R,k}$ have the same eigenvalues $\lambda_{k,m} = \lambda_m$, the last term in (11) is

$$N \log_2 \frac{\prod_{m=1}^M \lambda_m^{1/M}}{\lambda_M} \leq 0 \quad (12)$$

which contains the geometric mean of all eigenvalues divided by the largest eigenvalue. This ratio is smaller than one (or equal for uncorrelated channels) and thus its logarithm is negative and approaches $-\infty$ as the eigenvalue spread increases. In other words, Theorem 1 shows that BD has a (bounded) advantage on uncorrelated channels, while ZFC becomes the better choice as the receive-side correlation grows. The explanation is that BD has less restrictive interference mitigation, but is more sensitive to poor channels since it uses all channel dimensions for transmission. Therefore, we can expect a similar impact of any channel property that increases the eigenvalue spread in $\mathbf{H}_k \mathbf{H}_k^H$. This could for example be spatial correlation at the transmitter-side or a strong (low-rank) line-of-sight component.

To illustrate the opposite effect of having users with different path losses, we assume for simplicity that there are $\frac{N}{M}$ strong users with $\mathbf{R}_{R,k} = \gamma \mathbf{I}_M$, for some $\gamma > 1$, and $N - \frac{N}{M}$ weak users with $\mathbf{R}_{R,k} = \mathbf{I}_M$. If BD only serves the strong users while ZFC serves also the weak users, the last term in (11) becomes

$$\left(N - \frac{N}{M} \right) \log_2(\gamma) \geq 0. \quad (13)$$

This expression approaches $+\infty$ as the difference γ between the strong and weak users grows. In other words, BD is better at utilizing heterogeneous user channel conditions as it requires fewer users to be close to the base station to achieve high sum rates. This benefit will naturally diminish if some fairness mechanism is introduced to guarantee quality of service to users with unfavorable path losses.

The expected asymptotic difference in sum rate, $\bar{\beta}_{\text{BD-ZFC}}$, can be transferred into a difference $-\frac{\bar{\beta}_{\text{BD-ZFC}}}{10N \log_{10}(2)}$ [dB] in

transmit power to achieve the same sum rate in the high-SNR regime [22]. Theorem 1 shows that ZFC requires more power than BD in uncorrelated scenarios or highly heterogeneous user conditions, while BD requires more power under spatial correlation with relatively homogenous user conditions.

A. Impact of User Selection

The comparison in Theorem 1 was based on random user selection of the maximal number of users ($\frac{N}{M}$ with BD and N with ZFC), although scheduling of spatially separated users is necessary to achieve the full potential of multi-user MIMO. This paper assumes $K \geq N$ users, meaning that only a subset of users is scheduled at each channel use. If the users are unevenly distributed in the cell, it could be beneficial to intentionally schedule fewer users than possible. We will now analyze how the ability of selecting users with spatially compatible channels impacts performance.

In the high SNR regime, the optimal (semi-unitary) precoding matrix \mathbf{W}_k^{su} for single-user transmission matches the channel as $\tilde{\mathbf{C}}_k^H \mathbf{H}_k \mathbf{W}_k^{\text{su}} = \tilde{\mathbf{C}}_k^H \mathbf{H}_k$, while the precoding matrix $\mathbf{W}_k \in \mathbb{C}^{N \times d_k}$ of an SDMA scheme is also adapted to the co-user channels. The expected asymptotic performance loss of having to cancel inter-user interference is therefore

$$\begin{aligned} \mathbb{E}\{\text{Loss}\} &= \mathbb{E}\{\log_2 \det(\tilde{\mathbf{C}}_k^H \mathbf{H}_k \mathbf{H}_k^H \tilde{\mathbf{C}}_k) \\ &\quad - \log_2 \det(\tilde{\mathbf{C}}_k^H \mathbf{H}_k \mathbf{W}_k \mathbf{W}_k^H \mathbf{H}_k^H \tilde{\mathbf{C}}_k)\} \\ &= \mathbb{E}\left\{ \log_2 \frac{\det(\mathbf{\Lambda}_k \mathbf{\Lambda}_k^H)}{\det(\mathbf{\Lambda}_k \mathbf{B}_k \mathbf{W}_k \mathbf{W}_k^H \mathbf{B}_k^H \mathbf{\Lambda}_k^H)} \right\} \\ &= -\mathbb{E}\{\log_2 \det(\mathbf{B}_k \mathbf{W}_k \mathbf{W}_k^H \mathbf{B}_k^H)\} \end{aligned} \quad (14)$$

where $\mathbf{\Lambda}_k \in \mathbb{C}^{d_k \times d_k}$ contains the non-zero singular values of $\tilde{\mathbf{C}}_k^H \mathbf{H}_k$ and \mathbf{B}_k contains the corresponding right singular vectors.⁴ Observe that the eigenvalues of $\mathbf{B}_k \mathbf{W}_k \mathbf{W}_k^H \mathbf{B}_k^H$ are smaller or equal to one, thus $\mathbb{E}\{\text{Loss}\} \geq 0$. The following theorem shows how this loss is affected by user selection.

Theorem 2. For any given scheduling sets $\mathcal{S}^{\text{BD}}, \mathcal{S}^{\text{ZFC}}$ (with $|\mathcal{S}^{\text{BD}}| = \frac{N}{M}$ and $|\mathcal{S}^{\text{ZFC}}| = N$), suppose we replace one of the users in each set with the best one among K random users. If the best user is the one minimizing the expected asymptotic loss in (14), these losses for BD and ZFC, respectively, can be lower bounded as

$$\begin{aligned} \mathbb{E}\{\text{Loss}_{\text{BD}}\} &\geq -M \log_2(1 - c_1 K^{-\frac{1}{M(N-M)}}) \\ \mathbb{E}\{\text{Loss}_{\text{ZFC}}\} &\geq -\log_2(1 - c_2 K^{-\frac{1}{N-M}}) \end{aligned} \quad (15)$$

when K is large (c_1, c_2 are positive constants, see the proof).

Proof: The proof is given in Appendix C. ■

This theorem indicates that it is easier to find users with near-orthogonal channels under ZFC than under BD, which is reasonable since the random channels of BD users occupy M dimensions and should happen to be compatible to the other users in all these dimensions, while ZFC users only have one random dimension (and can adapt it using receive combining).

⁴These matrices can be obtained from a compact singular value decomposition $\tilde{\mathbf{C}}_k^H \mathbf{H}_k = \mathbf{U}_k \mathbf{\Lambda}_k \mathbf{B}_k$. Note that \mathbf{B}_k contains an orthonormal basis of the row space of the effective channel $\tilde{\mathbf{C}}_k^H \mathbf{H}_k$.

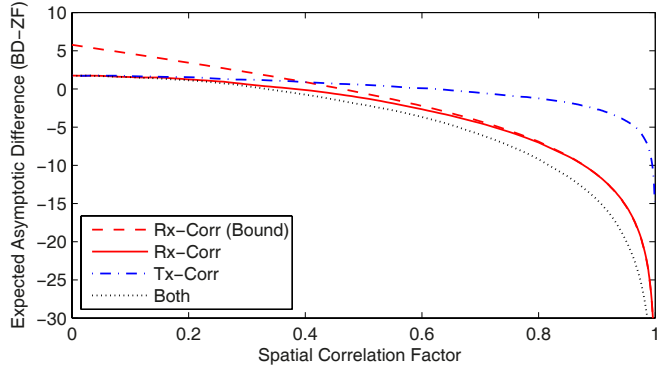


Fig. 3. The expected asymptotic difference between BD and ZFC in a system with $N = 8$ transmit antennas, $M = 2$ receive antennas per user, and random user selection. The impact of spatial correlation at the receiving users, transmitting base station, and both sides is shown (using the exponential correlation model from [24] with different correlation factors ρ).

B. Numerical Illustrations under Perfect CSI

Next, the analytic properties in Theorem 1 and Theorem 2 are illustrated numerically. To this end, we adopt the simple exponential correlation model of [24], where $0 \leq \rho \leq 1$ and

$$[\mathbf{R}(\rho, \theta)]_{ij} = \begin{cases} (\rho e^{i\theta})^{j-i}, & i \leq j, \\ (\rho e^{-i\theta})^{i-j}, & i > j, \end{cases} \quad \theta \sim U[0, 2\pi]. \quad (16)$$

The magnitude ρ is the *correlation factor* between adjacent antennas, where $\rho = 0$ means no spatial correlation and $\rho = 1$ means full correlation. For simplicity, all users have the same correlation factor (but θ is different). It is worth noting that ρ impacts the perceived spatial correlation non-linearly; a typical angular spread at a highly spatially correlated transmitter/receiver is 10-20 degrees which roughly corresponds to $\rho \approx 0.9$ [25].

The expected asymptotic difference between BD and ZFC is shown in Fig. 3 as a function of ρ , using $N = 8$ transmit antennas and $M = 2$ receive antennas. This simulation confirms that BD is advantageous in uncorrelated systems, while ZFC becomes beneficial as the correlation increases ($\rho > 0.4$ under receive-side correlation, $\rho > 0.7$ under transmit-side correlation, and $\rho > 0.25$ when both sides are correlated). The bound in Theorem 1 is only tight at high correlation.

To exemplify the impact of user selection, we use the *capacity-based suboptimal user selection* (CBSUS) algorithm from [26], which greedily adds users sequentially to maximize the sum rate and might give scheduling sets with fewer than N data streams. We consider a scenario with $N = 8$ uncorrelated transmit antennas and $M = 4$ receive antennas with correlation factor $\rho \in \{0, 0.4, 0.8\}$; see [27] for another scenario. We compare ZFC (1 stream/user) and BD (4 streams/user) with multi-user eigenmode transmission (MET) from [10] where data streams are allocated greedily with zero inter-user interference and users can have different number of streams. We also simulated 2 streams/user, but the result was always in between ZFC and BD is therefore not shown. Observe that all strategies might transmit fewer than N data streams.

Fig. 4 shows the average achievable sum rate as a function of the total number of users K . We consider the case when

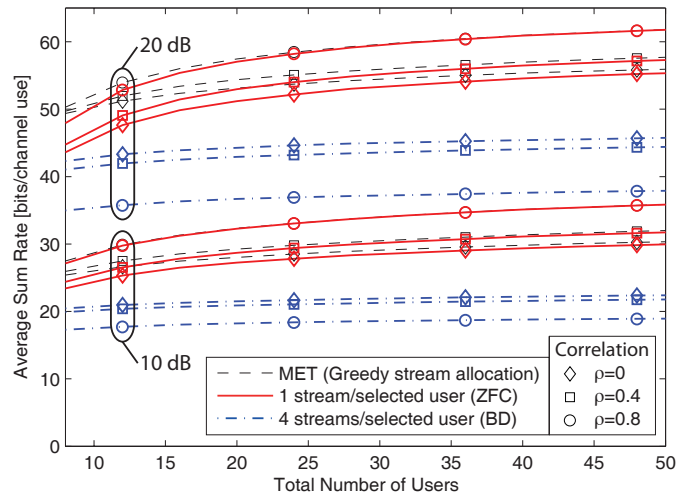


Fig. 4. The average achievable sum rate in a system with perfect CSI, $N = 8$ transmit antennas, $M = 4$ receive antennas, and the same average SNR among all users (10 or 20 dB). The performance with different strategies are shown as a function of the total number of users and for different correlation factors ρ among the receive antennas.

all users have the same average SNR (defined as $P \frac{\mathbb{E}\{\|\mathbf{H}_k\|^2\}}{NM}$), either equal to 10 or 20 dB. Irrespectively of the SNR, number of users, and receive-side correlation, ZFC outperforms BD. Thus, the scheduling-benefit of ZFC (from Theorem 2) dominates over the interference mitigation-benefit of BD (from Theorem 1)—even for spatially uncorrelated channels. As expected, the performance with ZFC improves with ρ , while correlation degrades the BD performance. MET has an advantages over ZFC since it can allocate different numbers of streams to different users (based on how many singular values are strong in their channels), but this advantage is small and disappears asymptotically with the number of users (as also noted in [10]).

Next, we consider heterogeneous conditions by having uniformly distributed users in a circular cell with radius 250 m (minimal distance is 35 m), a path loss coefficient of 3.5, and log-normal shadow-fading with 8 dB standard deviation. The average achievable sum rate is shown in Fig. 5 with an SNR of 20 dB at the cell edge.⁵ The variable path loss makes the results very different from the previous scenario. At low receive-correlation, BD outperforms ZFC, but the difference reduces with K . ZFC is however better than BD at high correlation and many users. MET has a large advantage over the other strategies, explained by its flexible stream allocation. To comprehend the difference, the probability that a selected user is allocated a certain number of streams is illustrated in Fig. 6. Spatial correlation reduces the number of streams per user, but the distance-dependence is even more significant; cell center users usually receive many streams while cell edge users only receive one or a few streams. This is natural since cell center users are more probable to have multiple relatively strong singular directions.

The conclusion is that ZFC is the method of choice in multi-user MIMO systems with perfect CSI and homogenous

⁵Such SNRs are reasonable in dense cellular systems and are necessary to compare BD and ZFC in regimes where these are supposed to work well.

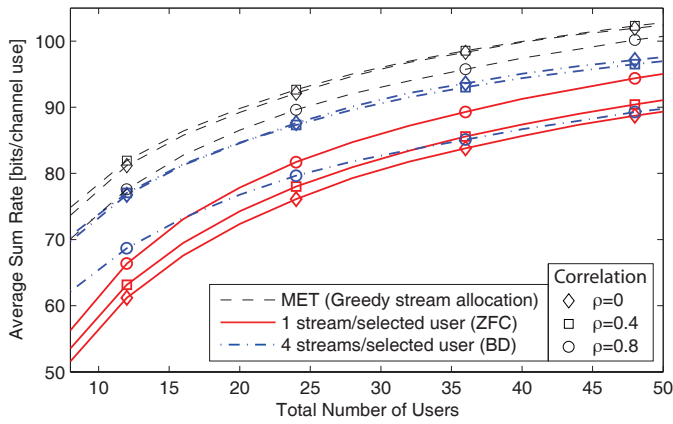


Fig. 5. The average achievable sum rate in a circular cell with perfect CSI, $N = 8$ transmit antennas, $M = 4$ receive antennas, and an SNR of 20 dB at the cell edge. The performance with different strategies are shown as a function of the total number of users and for different correlation factors ρ among the receive antennas.

user conditions (since it performs very closely to the more complicated MET). On the other hand, MET and BD are better under heterogeneous user conditions. It is worth noting that the more streams allocated per user, the more channel dimensions need to be known at the base station. The next section will therefore study how practical CSI acquisition affects our results.

IV. COMPARISON OF BD AND ZFC WITH IMPERFECT CSI

In this section, we continue the comparison of BD and ZFC by introducing imperfect CSI, originating from either quantized feedback in an FDD system or imperfect reverse-link estimation in a TDD system. The resources for channel acquisition are limited which has a major impact on both the number of channel dimensions that can be acquired per user and the accuracy of the acquired CSI. Theoretically, users can feed back different number of channel dimensions depending on some kind of long-term statistical CSI, but that would reduce the coverage (by favoring cell center users) and require a flexible system operation with additional control signaling. We therefore assume that the system acquires d dimensions/user from a randomly selected user set, where $d \geq 1$ is fixed but depends on the intended precoding strategy. This assumption is relaxed in the numerical evaluation.

A. Comparison with Quantized CSI

In the FDD system operation of Fig. 2(a), each user selected for feedback conveys the d -dimensional subspace spanned by its effective channel $\tilde{\mathbf{C}}_k^H \mathbf{H}_k$ using B bits. Similar to [6], [28]–[31], we use a codebook $\mathcal{C}_{N,d,B} = \{\mathbf{U}_1, \dots, \mathbf{U}_{2^B}\}$ with codewords $\mathbf{U}_i \in \mathbb{C}^{N \times d}$ from the (complex) *Grassmannian manifold* $\mathcal{G}_{N,d}$; that is, the set of all d -dimensional linear subspaces (passing through the origin) in an N -dimensional space. Each codeword forms an orthonormal basis, thus \mathbf{U}_i is a semi-unitary matrix satisfying $\mathbf{U}_i^H \mathbf{U}_i = \mathbf{I}_d$. User k selects the codeword that minimizes the chordal distance [32]:

$$\bar{\mathbf{H}}_k = \arg \min_{\mathbf{U} \in \mathcal{C}_{N,d,B}} \delta(\tilde{\mathbf{C}}_k^H \mathbf{H}_k, \mathbf{U}) \quad (17)$$

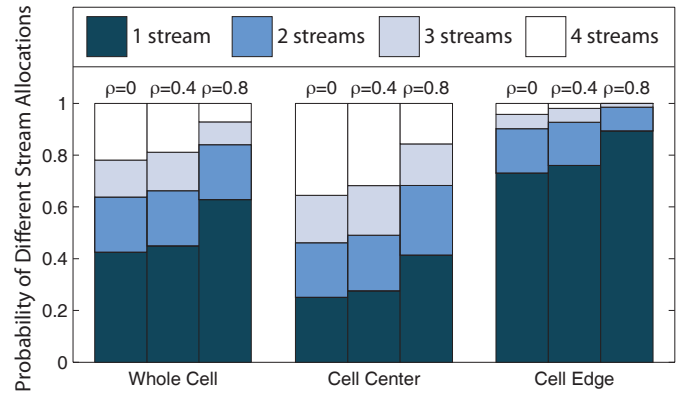


Fig. 6. The probability that a selected user is allocated a certain number of streams, assuming a circular cell with perfect CSI, $N = 8$ transmit antennas, $M = 4$ receive antennas, $K = 20$ users, and an SNR of 20 dB at the cell edge. The whole cell has a radius of 250 meters, whereof users closer than 100 meters belong to the cell center and users further than 200 meters belong to the cell edge.

where $\delta(\mathbf{B}, \mathbf{U}) = \sqrt{d - \text{tr}\{\text{span}\{\mathbf{B}\}^H \mathbf{U} \mathbf{U}^H \text{span}\{\mathbf{B}\}\}}$ and $\text{span}\{\cdot\}$ gives a matrix containing an orthonormal basis of the row space. We assume error-free and delay-free feedback, but the conclusions of this section are expected to hold true also under feedback errors (cf. [19]).

There is a variety of ways to handle feedback errors (especially if the error structure is known), but a simple approach is to treat $\bar{\mathbf{H}}_k$ as being the true channel [6] and calculate the precoding using a strategy developed for perfect CSI. This results in a lower bound on the performance and the information rates with BD and ZFC becomes

$$g_k^{\text{BD-Q}}(P) = \log_2 \frac{\det\left(\mathbf{I}_M + \sum_{\ell \in \mathcal{S}^{\text{BD}}} \mathbf{H}_k \bar{\mathbf{W}}_\ell^{\text{BD}} \bar{\mathbf{Y}}_\ell \bar{\mathbf{W}}_\ell^{\text{BD},H} \mathbf{H}_k^H\right)}{\det\left(\mathbf{I}_M + \sum_{\ell \in \mathcal{S}^{\text{BD}} \setminus \{k\}} \mathbf{H}_k \bar{\mathbf{W}}_\ell^{\text{BD}} \bar{\mathbf{Y}}_\ell \bar{\mathbf{W}}_\ell^{\text{BD},H} \mathbf{H}_k^H\right)} \quad (18)$$

$$g_k^{\text{ZFC-Q}}(P) = \log_2 \left(1 + \frac{\bar{p}_k |\mathbf{c}_k^H \mathbf{H}_k \bar{\mathbf{w}}_k^{\text{ZFC}}|^2}{1 + \sum_{\ell \in \mathcal{S}^{\text{ZFC}} \setminus \{k\}} \bar{p}_\ell |\mathbf{c}_\ell^H \mathbf{H}_k \bar{\mathbf{w}}_\ell^{\text{ZFC}}|^2}\right) \quad (19)$$

for users in the scheduling sets \mathcal{S}^{BD} and \mathcal{S}^{ZFC} , respectively.

Next, we quantify the performance loss for BD and ZFC compared with having perfect CSI. Random vector quantization (RVQ) is used for analytic convenience (as in [6], [7], [33], [34]), meaning that we average over codebooks with random codewords from the Grassmannian manifold. As any judicious codebook design is better than RVQ, the upper bounds on the performance loss that we will derive are valid for any reasonable codebook. The following theorem provides an upper bound on the performance loss under BD and extends results in [6] to include heterogeneous user conditions and spatial correlation.

Theorem 3. Assume that $\frac{N}{M}$ users are scheduled randomly. The average rate loss with BD (using equal power allocation) for user $k \in \mathcal{S}^{\text{BD}}$ due to RVQ is upper bounded as

$$\begin{aligned} \Delta_k^{\text{BD-Q}} &= \mathbb{E}\{g_k^{\text{BD}}(P) - g_k^{\text{BD-Q}}(P)\} \\ &\leq \log_2 \det\left(\mathbf{I}_M + \frac{P}{M} \mathbf{D}^{\text{BD}} \mathbf{R}_{R,k}\right) \end{aligned} \quad (20)$$

where the average quantization distortion is

$$D^{\text{BD}} = \mathbb{E}\{\delta^2(\mathbf{H}_k, \bar{\mathbf{H}}_k)\} \\ \approx \frac{\Gamma\left(\frac{1}{M(N-M)}\right)}{M(N-M)} \left(\frac{2^B}{(M(N-M))!} \prod_{i=1}^M \frac{(N-i)!}{(M-i)!} \right)^{-\frac{1}{M(N-M)}}. \quad (21)$$

Proof: The proof is given in Appendix D. ■

This theorem will be compared with the corresponding result for ZFC, but before stating that theorem we discuss how to select the (preliminary) receive combiner $\tilde{\mathbf{c}}_k$. There are primarily two factors to consider when selecting $\tilde{\mathbf{c}}_k$: the gain of the effective channel $\|\tilde{\mathbf{c}}_k^H \mathbf{H}_k\|_2^2$ and the quantization distortion. The results of [35], [36] indicate that the top priority in multi-user MIMO systems is to achieve small quantization errors. The error can be minimized by the *quantization-based combining* (QBC) approach in [7], where the codeword and receive combiner are selected jointly as

$$(\tilde{\mathbf{c}}_k^{\text{QBC}}, \bar{\mathbf{h}}_k) = \arg \max_{\substack{\mathbf{c}: \|\mathbf{c}\|_2=1 \\ \mathbf{u} \in \mathcal{C}_{N,1,B}}} \delta(\mathbf{H}_k^H \mathbf{c}, \mathbf{u}). \quad (22)$$

The *maximum expected SINR combiner* (MESC) in [8] achieves better practical performance by balancing effective channel gain and quantization distortion, but is asymptotically equal to QBC at high SNR. Since this is the regime of interest herein, we will exploit the analytic simplicity of QBC. Observe that QBC and MESC are only used for improved feedback accuracy; the MMSE combiner in Section II-A is used to maximize the performance during transmission (this was *not* done in the original QBC framework of [7]).

The following theorem provides an upper bound on the performance loss under ZFC and extends results in [7] to include heterogeneous user conditions and spatial correlation.

Theorem 4. Assume that $\mathbf{R}_{R,k}$ has eigenvalues $\lambda_{k,M} > \dots > \lambda_{k,1} > 0$ and that N users are selected randomly. The average rate loss for ZFC (using equal power allocation and the same $\tilde{\mathbf{c}}_k^{\text{QBC}}$) due to RVQ is upper bounded as

$$\Delta_k^{\text{ZFC-Q}} = \mathbb{E}\{g_k^{\text{ZFC}}(P) - g_k^{\text{ZFC-Q}}(P)\} \\ \leq \log_2 \left(1 + \frac{P}{N} D^{\text{QBC}} G_k \right) \quad (23)$$

where the average quantization distortion is

$$D^{\text{QBC}} = \mathbb{E}\{\delta^2(\mathbf{h}_k, \bar{\mathbf{h}}_k)\} \approx 2^{-\frac{B}{N-M}} \left(\frac{N-1}{M-1} \right)^{-\frac{1}{N-M}} \quad (24)$$

and the average channel gain with QBC is (where $\mu_n = \frac{1}{\lambda_{k,n}}$)

$$G_k = \sum_{m=1}^{M-1} \sum_{n=1}^m \sum_{t=m+1}^M \frac{(N-M+1)A_{m,n,t}}{(\mu_n - \mu_t) \prod_{\substack{i=1 \\ i \neq n}}^m (\mu_n - \mu_i) \prod_{\substack{j=m+1 \\ j \neq t}}^M (\mu_j - \mu_t)}, \\ A_{m,n,t} = \log_e \left(\frac{\mu_{m+1}}{\mu_m} \right) \frac{\mu_m^{m-1}}{(-\mu_t)^{2+m-M}} (m\mu_t + \mu_n(M-m-1)) \\ + \sum_{s=0}^{m-1} \sum_{r=0}^{M-m-1} \binom{m}{s} \binom{M-m-1}{r} \frac{\mu_n^{m-s} (-\mu_t)^{M-m-1-r}}{(-1)^s (1+s+r)} \\ \times \left(\frac{m-s}{\mu_n} + \frac{M-m-1-r}{\mu_t} \right) (\mu_m^{r+s} - \mu_{m+1}^{r+s}). \quad (25)$$

Proof: The proof is given in Appendix E. ■

The rate loss expressions in Theorem 3 and Theorem 4 for BD and ZFC, respectively, indicate the joint impact of spatial correlation (at the receiver) and CSI quantization on the performance. The main observation is that spatial correlation only has a marginal effect on the feedback accuracy; the expressions have a similar structure as for uncorrelated channels and the same scaling in the number of feedback bits is necessary to achieve the optimal multiplexing gain [6], [7].

Corollary 1. To achieve the optimal multiplexing gain with BD or ZFC under quantized CSI and arbitrary receive correlation, it is sufficient to scale the total number of CDI feedback bits for the scheduled users as

$$B_{\text{tot}} \approx N(N-M) \log_2(P) + \mathcal{O}(1). \quad (26)$$

While this corollary only provides a sufficient condition, we can expect the scaling law in (26) to also be necessary.⁶ It might seem unreasonable that the number of feedback bits should approach infinity with the SNR, but if we can achieve the optimal multiplexing gain in the downlink it is typically achievable also in the uplink [19]. Therefore, the uplink sum rate behaves as $N \log_2(P) + \mathcal{O}(1)$ and it is sufficient to allocate (approximately) $N-M$ channel uses for CSI feedback.

Observe that this result is based on random user selection, while additional feedback of gain information is necessary to achieve multi-user diversity or short-term rate adaptation (cf. [38]). As BD requires M times more bits per user, ZFC can typically achieve feedback from M times more users. We therefore expect ZFC to further strengthen its advantage at finding near-orthogonal users (proved in Theorem 2 under perfect CSI). In addition, spatial correlation at the transmitter-side (and other factors that make the channel matrices ill-conditioned) will inflict larger performance losses on BD than ZFC, just as in the case of perfect CSI.

B. Comparison under Estimated CSI

Next, we assume that the base station acquires CSI through imperfect CSI estimation. The primary focus will be on TDD systems, where channel estimates are obtained through training

⁶The necessary scaling can be proved for ZFC with QBC using a technique from [37, Theorem 4], while simulations in [6] shows that quantized ZFC and BD has the same scaling in the necessary number of bits.

signaling in the uplink (assuming perfect channel reciprocity). But it is worth noting that this approach is similar to having analog CSI feedback in FDD systems, where the unquantized channel coefficients are sent on an uplink subcarrier [6], [19].⁷

The reciprocal uplink counterpart to the system model in (2) is

$$\tilde{\mathbf{y}}_k = \mathbf{H}_k^T \tilde{\mathbf{x}}_k + \tilde{\mathbf{n}}_k \quad (27)$$

where $\tilde{\mathbf{y}}_k \in \mathbb{C}^{N \times 1}$ is the received uplink signal, $\tilde{\mathbf{x}}_k \in \mathbb{C}^{M \times 1}$ is the transmitted uplink signal, and $\tilde{\mathbf{n}}_k \sim \mathcal{CN}(\mathbf{0}, \sigma^2 \mathbf{I}_N)$ is the noise vector.⁸ To estimate $\tilde{\mathbf{C}}_k^H \mathbf{H}_k \in \mathbb{C}^{d \times N}$, user k sends $\tilde{\mathbf{C}}_k^* \mathbf{T}_k$ over d uplink channel uses, for some known training matrix $\mathbf{T}_k \in \mathbb{C}^{d \times d}$ and where $(\cdot)^*$ denotes complex conjugate. Assuming perfect statistical CSI, the MMSE estimate $\hat{\mathbf{H}}_k$ of $\tilde{\mathbf{C}}_k^H \mathbf{H}_k$ and the corresponding error covariance matrix \mathbf{E}_k are [18]

$$\begin{aligned} \text{vec}(\hat{\mathbf{H}}_k^T) &= \frac{1}{\sigma^2} \mathbf{E}_k \tilde{\mathbf{T}}_k^H \text{vec}(\mathbf{Y}_k), \\ \mathbf{E}_k &= \left((\tilde{\mathbf{C}}_k^H \mathbf{R}_{R,k} \tilde{\mathbf{C}}_k \otimes \mathbf{I}_N)^{-1} + \frac{\tilde{\mathbf{T}}_k^H \tilde{\mathbf{T}}_k}{\sigma^2} \right)^{-1} \end{aligned} \quad (28)$$

where $\tilde{\mathbf{T}}_k = (\mathbf{T}_k^T \otimes \mathbf{I}_N)$ and \mathbf{Y}_k is the received signal from training signaling. The training matrix \mathbf{T}_k has a total training power constraint $\text{tr}\{\mathbf{T}_k^H \mathbf{T}_k\} = \Psi$.

As under quantized CSI, we calculate the precoding by treating $\hat{\mathbf{H}}_k$ as the true channel. This results in a lower bound on the performance and the information rates with BD and ZFC becomes

$$g_k^{\text{BD-EST}}(P) = \log_2 \frac{\det\left(\mathbf{I}_M + \sum_{\ell \in \mathcal{S}^{\text{BD}}} \mathbf{H}_k \widehat{\mathbf{W}}_\ell^{\text{BD}} \hat{\mathbf{Y}}_\ell \widehat{\mathbf{W}}_\ell^{\text{BD},H} \mathbf{H}_k^H\right)}{\det\left(\mathbf{I}_M + \sum_{\ell \in \mathcal{S}^{\text{BD}} \setminus \{k\}} \mathbf{H}_k \widehat{\mathbf{W}}_\ell^{\text{BD}} \hat{\mathbf{Y}}_\ell \widehat{\mathbf{W}}_\ell^{\text{BD},H} \mathbf{H}_k^H\right)} \quad (29)$$

$$g_k^{\text{ZFC-EST}}(P) = \log_2 \left(1 + \frac{\hat{p}_k |\mathbf{c}_k^H \mathbf{H}_k \widehat{\mathbf{w}}_k^{\text{ZFC}}|^2}{1 + \sum_{\ell \in \mathcal{S}^{\text{ZFC}} \setminus \{k\}} \hat{p}_\ell |\mathbf{c}_k^H \mathbf{H}_k \widehat{\mathbf{w}}_\ell^{\text{ZFC}}|^2} \right) \quad (30)$$

for users in the scheduling sets \mathcal{S}^{BD} and \mathcal{S}^{ZFC} , respectively. The following theorem provides an upper bound on the performance loss under BD due to imperfect CSI estimation.

Theorem 5. Assume that $\frac{N}{M}$ users are scheduled randomly under BD. The average rate loss for user $k \in \mathcal{S}^{\text{BD}}$ (using equal power allocation) due to CSI estimation is upper bounded as

$$\begin{aligned} \Delta^{\text{BD}} &= \mathbb{E}\{g_k^{\text{BD}}(P) - g_k^{\text{BD-EST}}(P)\} \\ &\leq \log_2 \det \left(\mathbf{I}_M + \frac{P(N-M)}{N} \left(\mathbf{R}_{R,k}^{-T} + \frac{\mathbf{T}_k^H \mathbf{T}_k}{\sigma^2} \right)^{-1} \right). \end{aligned} \quad (31)$$

⁷Digital/quantized feedback might be beneficial over analog/unquantized feedback when there is plenty of resources for channel estimation [19]. But if very accurate CSI is required, Corollary 1 shows that the quantization codebooks grow very large and thus the search for the best codeword might be computationally infeasible.

⁸The downlink noise vector was normalized towards the channel matrix in the system model. To account for a different noise level at the base station, σ^2 is the (relative) uplink noise variance.

Proof: The proof is given in Appendix F. ■

This theorem will be compared with the corresponding result for ZFC, but before stating that theorem we need to consider the impact of having MRC as the receive combiner $\tilde{\mathbf{c}}_k$. ZFC is similar to applying BD to the effective channels $\mathbf{h}_k^H = \tilde{\mathbf{c}}_k^H \mathbf{H}_k$, but an important difference is that the effective channels are not Rayleigh fading (since $\tilde{\mathbf{c}}_k$ depends on the current channel realization). The expression in (28) will therefore not give the MMSE estimate, but fortunately the linear MMSE (LMMSE) estimator from a similar expression to (28) if we know the first two moments of \mathbf{h}_k [18].

Lemma 1. Assume that \mathbf{R}_R has eigenvalues $\lambda_M > \dots > \lambda_1 > 0$, where the user indices were dropped for convenience. If $\tilde{\mathbf{c}}$ is the dominating left singular vector of \mathbf{H} , it holds that

- the direction $\frac{\mathbf{h}}{\|\mathbf{h}\|_2}$ of $\mathbf{h} = \tilde{\mathbf{c}}^H \mathbf{H}$ is isotropically distributed on the unit sphere;
- the gain $\|\mathbf{h}\|_2^2$ is independent of the direction and

$$\begin{aligned} \mathbb{E}\{\|\mathbf{h}\|_2^2\} &= \sum_{m=1}^M \sum_{\zeta \in \mathcal{A}_M} \frac{\prod_{\ell=1}^M \lambda_{\zeta_\ell}^{N-\ell+1} \prod_{\ell=N-M+1}^N (\ell-1)!}{(-1)^{\text{per}(\zeta)+m+1} \det(\mathbf{\Delta})} \\ &\times \sum_{\beta \in \mathcal{B}_{m,M}} \sum_{\ell=0}^{K_m(\beta)} \sum_{\tilde{k} \in \tilde{\Omega}_\ell^{(m)}} \frac{\ell!}{\tilde{k}_1! \dots \tilde{k}_m!} \frac{(\sum_{i=1}^m \lambda_{\zeta_{\beta_i}}^{-1})^{-(\ell+1)}}{\prod_{i=1}^m \lambda_{\zeta_{\beta_i}}^{\tilde{k}_i}}, \end{aligned} \quad (32)$$

where the ij th element of $\mathbf{\Delta} \in \mathbb{R}^{M \times M}$ is given by

$$[\mathbf{\Delta}]_{ij} = \lambda_j^{N-i+1} (N-i)!. \quad (33)$$

In (32), the set of all permutations of $\{1, \dots, M\}$ is denoted \mathcal{A}_M . The sign of a given permutation $\zeta = \{\zeta_1, \dots, \zeta_M\} \in \mathcal{A}_M$ is denoted $(-1)^{\text{per}(\zeta)}$, where $\text{per}(\cdot)$ is the number of inversions⁹ in the permuted sequence. Next, $\mathcal{B}_{l,M}$ is the collection of all subsets of \mathcal{A}_M with cardinality l and increasing elements (i.e., $\beta_1 < \dots < \beta_l$ for $\beta = \{\beta_1, \dots, \beta_l\} \in \mathcal{B}_{l,M}$). The upper bound in the summation over ℓ is $K_l(\beta) = \sum_{i=1}^l (N - \beta_i)$. Finally, $\tilde{\Omega}_\ell^{(l)}$ is the set of all l -length partitions $\{\tilde{k}_1, \dots, \tilde{k}_l\}$ of ℓ (i.e., $\sum_{i=1}^l \tilde{k}_i = \ell$) that satisfy $0 \leq \tilde{k}_i \leq N - \beta_i$:

$$\tilde{\Omega}_\ell^{(l)} = \left\{ \{\tilde{k}_1, \dots, \tilde{k}_l\} : \sum_{j=1}^l \tilde{k}_j = \ell, 0 \leq \tilde{k}_j \leq N - \beta_j \forall j \right\}. \quad (34)$$

Proof: The proof is given in Appendix G. ■

The following theorem provides an upper bound on the performance loss under ZFC due to imperfect CSI estimation.

Theorem 6. Assume that N users are scheduled randomly under ZFC and that MRC is applied. The average rate loss for user $k \in \mathcal{S}^{\text{ZFC}}$ due to CSI estimation is upper bounded as

$$\begin{aligned} \Delta^{\text{ZFC-EST}} &= \mathbb{E}\{g_k^{\text{ZFC}}(P) - g_k^{\text{ZFC-EST}}(P)\} \\ &\leq \log_2 \left(1 + \frac{P(N-1)}{N} \frac{1}{\mathbb{E}\{\|\mathbf{h}_k\|_2^2\}^{-1} + \frac{\Psi}{\sigma^2}} \right). \end{aligned} \quad (35)$$

⁹An inversion in a sequence is a pair of numbers that are in incorrect order (i.e., not in ascending order).

Proof: The proof is given in Appendix H. ■

The rate loss expressions in Theorem 5 and Theorem 6 indicate the joint impact of spatial correlation and channel estimation on the performance of BD and ZFC, respectively. BD is slightly more resilient to CSI uncertainty, since the BD expression contains $(N - M)$ where the ZFC expression has $(N - 1)$. But observe that the performance losses are calculated against the same precoding strategy with perfect CSI; we know from Section III that ZFC and BD have different preferable user conditions, making it hard to analytically conclude which strategy to use under imperfect CSI estimation. However, the important result is the following extension of [19] to spatially correlated scenarios with $M \geq 1$.

Corollary 2. To achieve the optimal multiplexing gain with BD or ZFC under imperfect CSI estimation and arbitrary receive correlation, it is sufficient to scale the training power Ψ as

$$\frac{P}{\Psi} \rightarrow \text{constant} < \infty \quad \text{when } P \rightarrow \infty. \quad (36)$$

This corollary says that the training power should increase linearly with the transmit power to achieve the optimal sum rate scaling. This is for example satisfied by setting the total training power to $\Psi = P$ under ZFC and $\Psi = MP$ under BD, which corresponds to the reasonable assumption of having the same average SNR in the downlink and in the uplink.¹⁰ The demands for higher CSI accuracy with increasing SNR is therefore automatically fulfilled by the reduced estimation errors. Observe that one uplink channel use is consumed per user antenna dimension that is estimated, thus creating a practical bound on how many user channels that can be estimated in block fading systems [19]. As ZFC only has one effective antenna per user, it can accommodate M times more users than BD on the same estimation overhead and thereby exploit multi-user diversity to a larger extent.

V. NUMERICAL ILLUSTRATIONS UNDER IMPERFECT CSI

This section consists of two parts. First, the numerical illustrations in Section III-B are continued under imperfect CSI estimation. Then, we analyze the performance behavior under quantized CSI.

A. Continuation of Section III-B under Estimated CSI

We continue the simulations in Section III-B by introducing imperfect CSI estimation. We use MSE-minimizing training matrices from [18, Theorem 1] and training power $\Psi = dP$ (for estimation of d dimensions/user). The CBSUS algorithm in [26] is modified¹¹ to include the average interference (due to CSI estimation errors) in the scheduling.

The average achievable sum rate is shown in Fig. 7 as a function of the number of users that we obtain CSI estimates for using ZFC (while BD only obtains channel estimates for

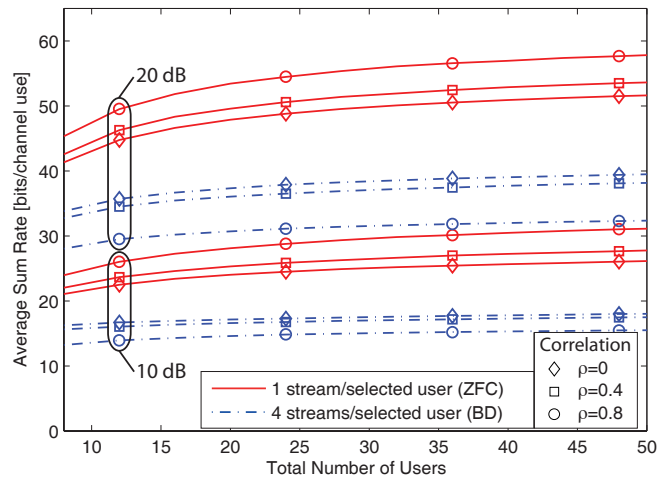


Fig. 7. The average achievable sum rate in a system with CSI estimation errors, $N = 8$ transmit antennas, $M = 4$ receive antennas, and the same average SNR among all users (10 or 20 dB). The performance with different strategies are shown as a function of the total number of users and for different correlation factors ρ among the receive antennas.

$\frac{1}{M}$ of them). All users have the same average SNR of either 10 or 20 dB. The performance loss compared with having perfect CSI is 10-20% (see Fig. 4), but the conclusion is otherwise the same and even clearer than before: ZFC outperforms BD in terms of performance with few users, in handling spatial correlation, and in exploiting multi-user diversity.

In case of a circular cell (see Section III-B for details), the average achievable sum rate is shown in Fig. 8. Recall from Fig. 5 that BD was often better than ZFC in this scenario under perfect CSI, but the case is completely different under imperfect CSI; ZFC outperforms the other strategies when the limited resources for CSI acquisition are taken into account. The explanation is that the ZFC benefit of easily finding near-orthogonal users (among M times more users than with BD) dominates the BD benefit of multi-stream multiplexing (preferably to cell center users). We also tested a MET-like scheme with greedy stream allocation (we took the optimum among feeding back 1, 2 or 4 channel dimensions per active user), but it was always identical to ZFC (in both Fig. 4 and Fig. 5)—this further confirms our conclusion.

The users selected for feedback were chosen randomly (e.g., in a round-robin fashion) in Figs. 7 and 8, but could theoretically be based on some kind of long-term statistical CSI. This could for instance mean that ZFC acquires one dimension from each of the K users, while BD acquires M dimensions from the $\frac{K}{M}$ users with the strongest long-term statistics $\text{tr}\{\mathbf{R}_{T,k}\}\text{tr}\{\mathbf{R}_{R,k}\}$. The greedy stream allocation strategy MET in [10] can be generalized to this scenario by finding the K strongest statistical eigendirections among the users and acquire CSI for an equivalent number of dimensions per user. Under these assumptions, the average achievable sum rate for the circular cell is shown in Fig. 9. The performance behavior is quite similar to the case with perfect CSI in Fig. 5; BD is better than ZFC, except at high correlation, and there is large gain from greedy stream allocation. However, we stress that this scenario is unrealistic as CSI is only acquired for cell

¹⁰Battery-powered user devices might operate at lower power than the base station, but Corollary 2 is satisfied as long as P and Ψ exhibit the same scaling. In practical scenarios, the path loss is the main source of SNR variations and affects the downlink and uplink equally.

¹¹Estimation errors contribute with an average interference of $P(|S| - 1)/|S|\mathbf{E}_{\text{est}}$, where $\mathbf{E}_{\text{est}} = (\mathbf{R}_{R,k}^{-T} + \mathbf{T}_k^H \mathbf{T}_k / \sigma^2)^{-1}$ for BD and $\mathbf{E}_{\text{est}} = (1/\mathbb{E}\{\|\mathbf{h}_k\|_2^2\} + \Psi/\sigma^2)^{-1}$ for ZFC.

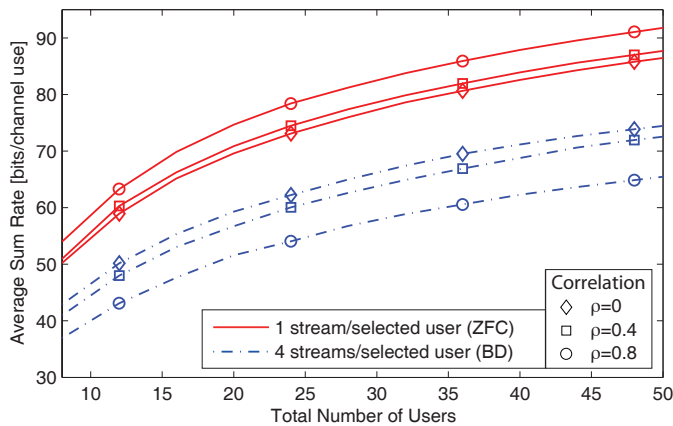


Fig. 8. The average achievable sum rate in a circular cell with CSI estimation errors, $N = 8$ transmit antennas, $M = 4$ receive antennas, and an SNR of 20 dB at the cell edge. The performance with different strategies are shown as a function of the total number of users and for different correlation factors ρ among the receive antennas.

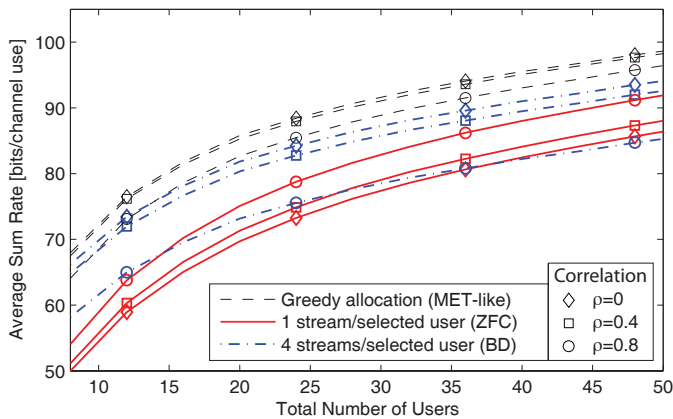


Fig. 9. The average achievable sum rate in a circular cell with CSI estimation errors, $N = 8$ transmit antennas, $M = 4$ receive antennas, and an SNR of 20 dB at the cell edge. The performance is shown as a function of the total number of users K , and CSI is only acquired for the users with strongest long-term statistics.

center users, thus reducing the coverage and user fairness as cell edge users are not even selected when their channels are relatively strong.

B. Observations under Quantized CSI

Next, we consider quantized CSI and let the number of feedback bits (per channel dimension) be scaled as $(N - M) \log_2(P) - \text{constant}$, where the constant is selected as in [6, Eq. (17)] to maintain a 3 dB gap between BD with perfect and quantized CSI. We consider $N = 4$ transmit antennas, $M = 2$ receive antennas, and RVQ. We also modify¹² the CBSUS algorithm in [26] to include the average interference due to quantization.

First, we compare BD (having either quantized or perfect CSI) with quantized ZFC using MESC-MMSE combining [8]

¹²Quantization errors contribute with an average interference of $P(|S| - 1)/|S| \mathbf{E}_{\text{quant}}$, where $\mathbf{E}_{\text{quant}} = N/(M(N - M)) D^{\text{BD}} \mathbf{R}_{R,k}$ for BD and $\mathbf{E}_{\text{quant}} = D^{\text{QBC}} G/(N - 1)$ for ZFC. When calculating D^{BD} and D^{QBC} , BD uses M times more feedback bits per user than ZFC.

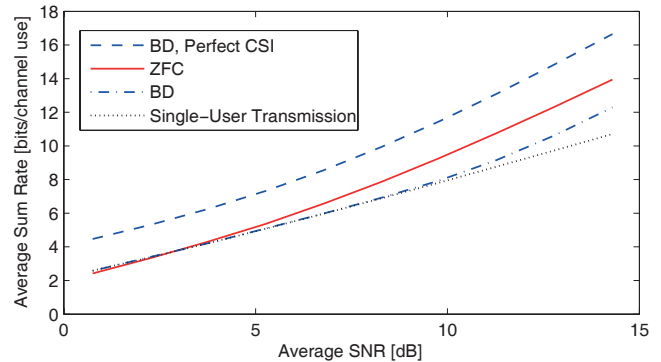


Fig. 10. The average achievable sum rate with BD and ZFC, quantized CSI feedback, $N = 4$ transmit antennas, $M = 2$ receive antennas, uncorrelated channels, and varying SNR. The number of feedback bits is scaled with the transmit power according to Corollary 1 and [6, Eq. (17)].

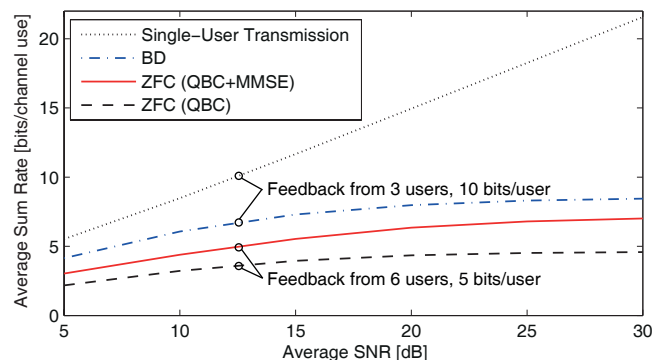


Fig. 11. Comparison of single-user transmission, BD, and different forms of ZFC under quantized CSI feedback. The scenario is the same as in [6, Fig. 6], where the superior single-user strategy was not included.

and with single-user SVD-based transmission (to a randomly selected user). The quantized effective channels are obtained from 8 users under ZFC, while the entire channels are quantized for 4 users under BD. The average achievable sum rate is shown in Fig. 10 as a function of the average SNR. At low SNR, quantized BD only selects one user and performs similar to single-user transmission. As two data streams are transmitted to the selected user, both strategies are slightly better than ZFC in this regime. But quantized ZFC quickly improves with SNR and becomes the method of choice at practical SNRs. The simulation was stopped at $P = 14.3$ dB where BD requires feedback of 22 bits per user, meaning that the best codeword is selected in a codebook with over a million entries.¹³ BD is therefore suboptimal both in terms of sum rate and computational complexity.

This observation stands in contrast to the numerical results in [6], where BD clearly beats ZFC under quantized CSI. To explain the difference, we repeat the simulation in [6, Fig. 6] with $N = 6$ transmit antennas and $M = 2$ receive antennas. In this simulation, the RVQ codebooks contain 10 bits/user under BD and 5 bits/user under ZFC. The achievable sum rate is shown in Fig. 11 for the quantized BD approach

¹³An approach to emulate RVQ for very large random codebooks was proposed in [6], but this does not change the fact that the quantization complexity becomes infeasible much faster under BD than under ZFC.

in [6] and the ZFC-QBC approach in [7]. We have also included: 1) an improved version of ZFC-QBC where the MMSE receive combiner is applied during transmission; and 2) single-user SVD-based transmission to a randomly selected user. Our simulation confirms that BD is better than ZFC in this scenario, but the difference becomes much smaller when the MMSE combiner is applied. However, none of these strategies should be used in this scenario since single-user transmission is vastly superior. The explanation is that the number of feedback bits is fixed at a number that only exceeds the feedback scaling law in (26) and [6, Eq. (17)] at low SNR (cf. [6, Fig. 2]), while the strict interference mitigation in BD and ZFC is only practically meaningful at high SNR. The observation in [6] is thus misleading.

Conclusions from the mathematical and numerical analysis are summarized in the next section.

VI. CONCLUSION

This paper analyzed how to divide data streams among users in a downlink system with many multi-antenna users; should few users be allocated many streams, or many users be allocated few streams? New and generalized analytic results were obtained to study this tradeoff under spatial correlation, user selection, heterogeneous user channel conditions, and practical CSI acquisition.

The main conclusion is that sending one stream per selected user and exploiting receive combining is the best choice under realistic conditions. This is good news as it reduces the hardware requirements at the users, compared with multi-stream multiplexing. The result is explained by a stronger resilience towards spatial correlation (Theorem 1) and larger benefit from user selection (Theorem 2). To arrive at alternative conclusions, one has to consider a scenario with heterogeneous user conditions with either perfect CSI (unrealistic) or where CSI is only acquired for the strongest users (destroys coverage and fairness). It should however be noted that if only very inaccurate CSI can be acquired, then inter-user interference will limit performance thus making single-user transmission advantageous.

APPENDIX A COLLECTION OF LEMMAS

This appendix contains two lemmas that are essential for proving the theorems of this paper. The first result shows how spatial correlation at the receiver affects the channel directions.

Lemma 2. Let $\mathbf{A} \succ \mathbf{0}_M$ be any Hermitian positive-definite matrix and let $\tilde{\mathbf{H}} \in \mathbb{C}^{M \times N}$ be an arbitrary matrix. Then, $\text{span}(\tilde{\mathbf{H}}) = \text{span}(\mathbf{A}\tilde{\mathbf{H}})$, where $\text{span}(\cdot)$ denotes the row space.

Proof: Let $\mathbf{A} = \mathbf{U}_A \mathbf{\Lambda}_A \mathbf{U}_A^H$ be an eigen decomposition of \mathbf{A} . The lemma follows by observing that \mathbf{U}_A only rotates the basis vectors of the row space and $\mathbf{\Lambda}_A$ scales the rows without affecting their span. ■

The second result generalizes the bounding of performance loss under imperfect CSI in [6], [7].

Lemma 3. Let $\mathbf{W}_k, \tilde{\mathbf{W}}_k$ be isotropically distributed on the Grassmannian manifold \mathcal{G}_{N,d_k} and independent of \mathbf{H}_k , then

$$\begin{aligned} & \mathbb{E} \left\{ \log_2 \det \left(\mathbf{I}_{d_k} + \frac{P}{N} \tilde{\mathbf{C}}_k^H \mathbf{H}_k \mathbf{W}_k \mathbf{W}_k^H \mathbf{H}_k^H \tilde{\mathbf{C}}_k \right) \right\} \\ & - \mathbb{E} \left\{ \log_2 \frac{\det \left(\mathbf{I}_{d_k} + \frac{P}{N} \sum_{\ell} \tilde{\mathbf{C}}_k^H \mathbf{H}_k \tilde{\mathbf{W}}_{\ell} \tilde{\mathbf{W}}_{\ell}^H \mathbf{H}_k^H \tilde{\mathbf{C}}_k \right)}{\det \left(\mathbf{I}_{d_k} + \frac{P}{N} \sum_{\ell \neq k} \tilde{\mathbf{C}}_k^H \mathbf{H}_k \tilde{\mathbf{W}}_{\ell} \tilde{\mathbf{W}}_{\ell}^H \mathbf{H}_k^H \tilde{\mathbf{C}}_k \right)} \right\} \\ & \leq \log_2 \det \left(\mathbf{I}_{d_k} + \frac{P}{N} \sum_{\ell \neq k} \mathbb{E} \left\{ \tilde{\mathbf{C}}_k^H \mathbf{H}_k \tilde{\mathbf{W}}_{\ell} \tilde{\mathbf{W}}_{\ell}^H \mathbf{H}_k^H \tilde{\mathbf{C}}_k \right\} \right). \end{aligned} \quad (37)$$

Proof: This lemma follows from two inequalities. First,

$$\begin{aligned} & \mathbb{E} \left\{ \log_2 \det \left(\mathbf{I}_{d_k} + \frac{P}{N} \tilde{\mathbf{C}}_k^H \mathbf{H}_k \mathbf{W}_k \mathbf{W}_k^H \mathbf{H}_k^H \tilde{\mathbf{C}}_k \right) \right\} \\ & - \mathbb{E} \left\{ \log_2 \det \left(\mathbf{I}_{d_k} + \frac{P}{N} \sum_{\ell} \tilde{\mathbf{C}}_k^H \mathbf{H}_k \tilde{\mathbf{W}}_{\ell} \tilde{\mathbf{W}}_{\ell}^H \mathbf{H}_k^H \tilde{\mathbf{C}}_k \right) \right\} \leq 0 \end{aligned} \quad (38)$$

since $\tilde{\mathbf{C}}_k^H \mathbf{H}_k \mathbf{W}_k \mathbf{W}_k^H \mathbf{H}_k^H \tilde{\mathbf{C}}_k$ and $\tilde{\mathbf{C}}_k^H \mathbf{H}_k \tilde{\mathbf{W}}_{\ell} \tilde{\mathbf{W}}_{\ell}^H \mathbf{H}_k^H \tilde{\mathbf{C}}_k$ have the same distribution, and the second term contains additional positive semi-definite matrices. Second, applying Jensen's inequality on the concave function $\log_2 \det(\cdot)$ gives

$$\begin{aligned} & \mathbb{E} \left\{ \log_2 \det \left(\mathbf{I}_{d_k} + \frac{P}{N} \sum_{\ell \neq k} \tilde{\mathbf{C}}_k^H \mathbf{H}_k \tilde{\mathbf{W}}_{\ell} \tilde{\mathbf{W}}_{\ell}^H \mathbf{H}_k^H \tilde{\mathbf{C}}_k \right) \right\} \\ & \leq \log_2 \det \left(\mathbf{I}_{d_k} + \frac{P}{N} \sum_{\ell \neq k} \mathbb{E} \left\{ \tilde{\mathbf{C}}_k^H \mathbf{H}_k \tilde{\mathbf{W}}_{\ell} \tilde{\mathbf{W}}_{\ell}^H \mathbf{H}_k^H \tilde{\mathbf{C}}_k \right\} \right). \end{aligned} \quad (39)$$

The lemma follows from combining (38) and (39). ■

APPENDIX B PROOF OF THEOREM 1

Using (10), the asymptotic difference can be expressed as

$$\beta = \log_2 \left(\frac{\prod_{k \in \mathcal{S}^{\text{BD}}} \det(\mathbf{H}_k \mathbf{W}_k^{\text{BD}} \mathbf{W}_k^{\text{BD},H} \mathbf{H}_k^H)}{\prod_{k \in \mathcal{S}^{\text{ZFC}}} |\tilde{\mathbf{c}}_k^H \mathbf{H}_k \mathbf{w}_k^{\text{ZFC}}|^2} \right). \quad (40)$$

Assume that $\tilde{\mathbf{c}}_k \in \mathbb{C}^{M \times 1}$ is selected suboptimally as the dominating eigenvector of $\mathbf{R}_{R,k}$. This is a lower bound because every judicious selection based on perfect CSI (e.g., MRC) achieves better performance, but it is convenient since $\tilde{\mathbf{c}}_k^H \mathbf{H}_k = \sqrt{\lambda_{k,M}} \tilde{\mathbf{h}}_k^H$ with $\tilde{\mathbf{h}}_k \sim \mathcal{CN}(\mathbf{0}, \mathbf{I}_N)$. The asymptotic difference can thus be upper bounded as

$$\begin{aligned} \beta & \leq \log_2 \left(\frac{\prod_{k \in \mathcal{S}^{\text{BD}}} \det(\tilde{\mathbf{H}}_k \mathbf{W}_k^{\text{BD}} \mathbf{W}_k^{\text{BD},H} \tilde{\mathbf{H}}_k^H)}{\prod_{k \in \mathcal{S}^{\text{ZFC}}} |\tilde{\mathbf{h}}_k^H \mathbf{w}_k^{\text{ZFC}}|^2} \right) \\ & + \sum_{k \in \mathcal{S}^{\text{BD}}} \log_2 \det(\mathbf{R}_{R,k}) - \sum_{k \in \mathcal{S}^{\text{ZFC}}} \log_2(\lambda_{k,M}). \end{aligned} \quad (41)$$

We have $\tilde{\beta}_{\text{BD-ZFC}} = \mathbb{E}\{\beta\}$ and the expectation of the first term of (41) can be rewritten as the first term in (11) by applying [22, Theorem 3]. The cited theorem was stated for uncorrelated channels, but can be applied in our scenario since \mathbf{W}_k^{BD} is not affected by the receive-side correlation matrices $\mathbf{R}_{R,\ell} \forall \ell \in \mathcal{S}^{\text{ZFC}}$; see Lemma 2 in Appendix A which shows that receive correlation will not affect the row space

of channels (i.e., the spaces where inter-user interference are canceled). Finally, observe that the last two terms of (41) are deterministic and correspond to the second term in (11).

APPENDIX C PROOF OF THEOREM 2

We begin with BD and assume that there are K candidates to become the new user k , $\mathcal{K} = \{1, \dots, K\}$, while the other users in \mathcal{S}^{BD} are fixed. Since $|\mathcal{S}^{\text{BD}}| = \frac{N}{M}$, all available degrees of freedom are consumed by the interference cancellation. The precoding matrix \mathbf{W}_k^{BD} is therefore completely determined by the common null space of the co-users' channels and fixed in this proof.

Minimizing (14) corresponds to finding the user $\ell \in \mathcal{K}$ with the row space of \mathbf{H}_ℓ most compatible with \mathbf{W}_k^{BD} . For a user candidate $\ell \in \mathcal{K}$, we can lower bound (14) as

$$\begin{aligned} & -\mathbb{E}\{\log_2 \det(\mathbf{B}_\ell \mathbf{W}_k^{\text{BD}} \mathbf{W}_k^{\text{BD},H} \mathbf{B}_\ell^H)\} \\ &= -M \mathbb{E}\{\log_2 (\det(\mathbf{B}_\ell \mathbf{W}_k^{\text{BD}} \mathbf{W}_k^{\text{BD},H} \mathbf{B}_\ell^H)^{1/M})\} \\ &\geq -M \mathbb{E}\left\{\log_2 \left(\frac{\text{tr}\{\mathbf{B}_\ell \mathbf{W}_k^{\text{BD}} \mathbf{W}_k^{\text{BD},H} \mathbf{B}_\ell^H\}}{M}\right)\right\} \\ &\geq -M \log_2 \left(\frac{\mathbb{E}\{\text{tr}\{\mathbf{B}_\ell \mathbf{W}_k^{\text{BD}} \mathbf{W}_k^{\text{BD},H} \mathbf{B}_\ell^H\}\}}{M}\right) \\ &= -M \log_2 \left(1 + \frac{\mathbb{E}\{\text{tr}\{\mathbf{B}_\ell \mathbf{W}_k^{\text{BD}} \mathbf{W}_k^{\text{BD},H} \mathbf{B}_\ell^H\} - M\}}{M}\right). \end{aligned} \quad (42)$$

The first inequality is the classic inequality between arithmetic and geometric means, while the second inequality follows from applying Jensen's inequality on the convex function $-\log_2 \det(\cdot)$. The final expression in (42) contains $M - \text{tr}\{\mathbf{B}_\ell \mathbf{W}_k^{\text{BD}} \mathbf{W}_k^{\text{BD},H} \mathbf{B}_\ell^H\}$, which is the squared chordal distance between \mathbf{B}_ℓ and \mathbf{W}_k^{BD} .

Since the matrices \mathbf{B}_ℓ , for $\ell \in \mathcal{K}$, are independent and isotropically distributed on the Grassmannian manifold $\mathcal{G}_{N,M}$ irrespectively of the receive-side correlation (see Lemma 2), we can bring in results from [29] on quantization of Grassmannian manifolds using K random codewords. From [29, Theorem 4], we have the following lower bound on the average squared chordal distance (for sufficiently large K):

$$\begin{aligned} & \min_{\ell \in \mathcal{K}} \mathbb{E}\left\{M - \text{tr}\{\mathbf{B}_\ell \mathbf{W}_k^{\text{BD}} \mathbf{W}_k^{\text{BD},H} \mathbf{B}_\ell^H\}\right\} \\ & \geq \frac{M(N-M)}{M(N-M)+1} c_{N,M,M,2}^{-\frac{1}{M(N-M)}} K^{-\frac{1}{M(N-M)}} \end{aligned} \quad (43)$$

where $c_{N,M,M,2}$ is a positive constant defined in [29, Eq. (8)]. Plugging (43) into (42) yields the lower bound for BD in the theorem.

A similar approach can be taken under ZFC (by setting $M = 1$ in the derivation), but the M receive antennas provide degrees of freedom to select the effective channel as the vector in the row space of \mathbf{H}_ℓ that minimizes the chordal distance to $\mathbf{w}_k^{\text{ZFC}}$. This is done by the QBC approach in [7], which was derived for uncorrelated channels but can be applied under receive correlation due to Lemma 2. We apply [7, Lemma 1],

which says that the minimal chordal distance is the minimum of K independent $\beta(N-M, M)$ -distributed random variables. This quantity can be lower bounded by taking the minimum of K independent $\beta(N-M, 1)$ variables and further lower bounded by the quantization bound in [29, Theorem 4]:

$$\min_{\ell \in \mathcal{K}} \mathbb{E}\left\{1 - \frac{|\mathbf{h}_\ell^H \mathbf{w}_k^{\text{ZFC}}|^2}{\|\mathbf{h}_\ell\|_2^2}\right\} \geq \frac{(N-M)K^{-\frac{1}{(N-M)}}}{(N-M)+1} c_{N-M+1,1,1,2}^{-\frac{1}{(N-M)}} \quad (44)$$

where $c_{N-M+1,1,1,2}$ is a positive constant defined in [29, Eq. (8)]. Plugging (44) into (42) (with $M = 1$) yields the lower bound for ZFC in the theorem.

APPENDIX D PROOF OF THEOREM 3

Using Lemma 2, the row space of the correlated channel $\mathbf{H}_k = \mathbf{R}_{R,k}^{1/2} \tilde{\mathbf{H}}_k$ is the same as for the uncorrelated channel $\tilde{\mathbf{H}}_k$. Consequently, $\bar{\mathbf{W}}_k^{\text{BD}}$ will be isotropically distributed on the Grassmannian manifold $\mathcal{G}_{N,M}$, just as for uncorrelated channels in [6, Theorem 1]. The performance loss can therefore be bounded using Lemma 3 and it only remains to characterize $\mathbb{E}\{\mathbf{H}_k \bar{\mathbf{W}}_\ell^{\text{BD}} \bar{\mathbf{W}}_\ell^{\text{BD},H} \mathbf{H}_k^H\}$ for $\ell \neq k$. Observe that

$$\begin{aligned} & \mathbb{E}\{\mathbf{H}_k \bar{\mathbf{W}}_\ell^{\text{BD}} \bar{\mathbf{W}}_\ell^{\text{BD},H} \mathbf{H}_k^H\} \\ &= \mathbf{R}_{R,k}^{1/2} \mathbb{E}\{\mathbf{L}_k \mathbf{Q}_k \bar{\mathbf{W}}_\ell^{\text{BD}} \bar{\mathbf{W}}_\ell^{\text{BD},H} \mathbf{Q}_k^H \mathbf{L}_k^H\} \mathbf{R}_{R,k}^{1/2,H} \end{aligned} \quad (45)$$

using that $\mathbf{H}_k = \mathbf{R}_{R,k}^{1/2} \tilde{\mathbf{H}}_k = \mathbf{R}_{R,k}^{1/2} \mathbf{L}_k \mathbf{Q}_k$, where $\mathbf{L}_k \in \mathbb{C}^{M \times M}$ is the lower triangular matrix and $\mathbf{Q}_k \in \mathbb{C}^{M \times N}$ is the semi-unitary matrix in an LQ decomposition of $\tilde{\mathbf{H}}_k$. Observe that \mathbf{L}_k and \mathbf{Q}_k are independent, thus we can calculate their expectations sequentially as

$$\begin{aligned} & \mathbb{E}\{\mathbf{L}_k \mathbf{Q}_k \bar{\mathbf{W}}_\ell^{\text{BD}} \bar{\mathbf{W}}_\ell^{\text{BD},H} \mathbf{Q}_k^H \mathbf{L}_k^H\} \\ &= \frac{D^{\text{BD}}}{N-M} \mathbb{E}\{\mathbf{L}_k \mathbf{I}_M \mathbf{L}_k^H\} = \frac{ND^{\text{BD}}}{N-M} \mathbf{I}_M. \end{aligned} \quad (46)$$

The first equality follows from [6, Eq. (43)-(45)], while the second follows from $\mathbb{E}\{\mathbf{L}_k \mathbf{L}_k^H\} = N \mathbf{I}_M$ (since $\mathbb{E}\{\tilde{\mathbf{H}}_k \tilde{\mathbf{H}}_k^H\} = N \mathbf{I}_M$). Plugging (46) into Lemma 3 yields

$$\Delta^{\text{BD}} \leq \log_2 \det \left(\mathbf{I}_M + \frac{P}{N} \left(\frac{N}{M} - 1 \right) \frac{ND^{\text{BD}}}{N-M} \mathbf{R}_{R,k} \right) \quad (47)$$

from which (20) follows directly. The approximate expression for D^{BD} is given in [6, Eq. (26)].

APPENDIX E PROOF OF THEOREM 4

This proof follows along the lines of [7, Theorem 1], with the difference that 1) we have spatial correlation at the receiver; and 2) we use QBC also under perfect CSI. Using Lemma 2, we observe that the row space of the correlated channel $\mathbf{H}_k = \mathbf{R}_{R,k}^{1/2} \tilde{\mathbf{H}}_k$ is the same as for the uncorrelated channel $\tilde{\mathbf{H}}_k$. Since the gain of the effective channel is ignored in (22), the error-minimizing codeword is the same as for uncorrelated channels and we can apply [7, Lemma 2] to conclude that the direction of the effective channel $\mathbf{h}_k = \mathbf{H}_k^H \tilde{\mathbf{c}}_k^{\text{QBC}}$ is isotropically distributed. The beamforming vector $\bar{\mathbf{w}}_k^{\text{ZFC}}$ is

independent of \mathbf{h}_k and also isotropic, thus the performance loss can be bounded using Lemma 3. It only remains to characterize $\mathbb{E}\{|\mathbf{h}_k^H \tilde{\mathbf{w}}_\ell^{\text{ZFC}}|^2\} = \mathbb{E}\{\|\mathbf{h}_k\|_2^2\} \mathbb{E}\{\|\frac{\mathbf{h}_k^H}{\|\mathbf{h}_k\|_2} \tilde{\mathbf{w}}_\ell^{\text{ZFC}}\}^2$ for $\ell \neq k$. The second factor equals $\frac{D^{\text{QBC}}}{N-1}$ using [37, Lemma 2] and [7, Eq. (17)], while the average norm $\mathbb{E}\{\|\mathbf{h}_k\|_2^2\}$ of the effective channel is nontrivial. To enable reuse of results from [7], let $\tilde{\mathbf{c}}_k^{\text{U-QBC}}$ be the QBC for the uncorrelated channel $\tilde{\mathbf{H}}_k$ and observe that

$$\tilde{\mathbf{c}}_k^{\text{QBC}} = \frac{\mathbf{R}_{R,k}^{-1/2} \tilde{\mathbf{c}}_k^{\text{U-QBC}}}{\|\mathbf{R}_{R,k}^{-1/2} \tilde{\mathbf{c}}_k^{\text{U-QBC}}\|_2}. \quad (48)$$

We can therefore express the effective channel as

$$\mathbf{h}_k = \mathbf{H}_k^H \tilde{\mathbf{c}}_k^{\text{QBC}} = \mathbf{H}_k^H \frac{\mathbf{R}_{R,k}^{-1/2} \tilde{\mathbf{c}}_k^{\text{U-QBC}}}{\|\mathbf{R}_{R,k}^{-1/2} \tilde{\mathbf{c}}_k^{\text{U-QBC}}\|_2} = \frac{\tilde{\mathbf{H}}_k^H \tilde{\mathbf{c}}_k^{\text{U-QBC}}}{\|\mathbf{R}_{R,k}^{-1/2} \tilde{\mathbf{c}}_k^{\text{U-QBC}}\|_2} \quad (49)$$

and its squared norm will be

$$\|\mathbf{h}_k\|_2^2 = \|\tilde{\mathbf{H}}_k^H \tilde{\mathbf{c}}_k^{\text{U-QBC}}\|_2^2 \frac{1}{\|\tilde{\mathbf{c}}_k^{\text{U-QBC},H} \mathbf{R}_{R,k}^{-1} \tilde{\mathbf{c}}_k^{\text{U-QBC}}\|_2}. \quad (50)$$

The first factor is the same as under uncorrelated fading and has $\mathbb{E}\{\|\tilde{\mathbf{H}}_k^H \tilde{\mathbf{c}}_k^{\text{U-QBC}}\|_2^2\} = N - M + 1$ (see [7, Lemma 4]), while the second factor depends on $\mathbf{R}_{R,k}$. Since both the quantization codebook and $\tilde{\mathbf{H}}_k$ are isotropically distributed, $\tilde{\mathbf{c}}_k^{\text{U-QBC}}$ is also isotropic and the two terms in (50) are independent. To characterize the second term, observe that $\tilde{\mathbf{c}}_k^{\text{U-QBC}}$ can be viewed as a normalized uncorrelated circular-symmetric complex Gaussian vector. By using that the eigenvectors of $\mathbf{R}_{R,k}$ are not affecting the distribution and that squared magnitudes of $\mathcal{CN}(0, 1)$ -variables are exponentially distributed [39], we conclude that the second term of (50) has the same distribution as

$$\frac{\sum_{i=1}^M \xi_i}{\sum_{i=1}^M \frac{\xi_i}{\lambda_{k,i}}} \quad (51)$$

for independent exponentially distributed $\xi_i \sim \text{Exp}(1)$. For any a such that $\lambda_{k,m} \leq a \leq \lambda_{k,m+1}$, we can write the CDF as

$$\begin{aligned} & \Pr \left\{ \frac{\sum_{i=1}^M \xi_i}{\sum_{i=1}^M \frac{\xi_i}{\lambda_{k,i}}} \leq a \right\} \\ &= \Pr \left\{ \sum_{i=1}^m \underbrace{\left(\frac{a}{\lambda_{k,i}} - 1 \right)}_{\geq 0} \xi_i - \sum_{i=m+1}^M \underbrace{\left(1 - \frac{a}{\lambda_{k,i}} \right)}_{\geq 0} \xi_i \geq 0 \right\}. \end{aligned} \quad (52)$$

This is the difference of two sums of exponentially distributed variables (with distinct positive variances). The PDF of each sum is characterized by [39, Theorem 4] and by calculating their convolution and integrating over all positive values, we

achieve the CDF

$$\begin{aligned} & \Pr \left\{ \frac{\sum_{i=1}^M \xi_i}{\sum_{i=1}^M \frac{\xi_i}{\lambda_{k,i}}} \leq a \right\} \\ &= \sum_{n=1}^m \sum_{t=m+1}^M \frac{(\mu_n - a^{-1})^m (a^{-1} - \mu_t)^{M-m-1}}{(\mu_n - \mu_t) \prod_{\substack{i=1 \\ i \neq n}}^m (\mu_n - \mu_i) \prod_{\substack{j=m+1 \\ j \neq t}}^M (\mu_j - \mu_t)} \end{aligned} \quad (53)$$

using the simplifying notation $\mu_n = \frac{1}{\lambda_{k,n}}$. The corresponding mean value is achieved from the CDF by simply taking the derivative and sum up the mean values over each a -interval. By multiplying the mean value expression with $N - M + 1$ (i.e., the contribution of the first part in (50)), we achieve the expression for G_k .

APPENDIX F PROOF OF THEOREM 5

The proof follows along the lines of Theorem 3, with the difference that we consider CSI estimation errors instead of quantization errors. First, observe that both $\mathbf{W}_\ell^{\text{BD}}$ and $\widehat{\mathbf{W}}_\ell^{\text{BD}}$ are isotropically distributed on the Grassmannian manifold $\mathcal{G}_{N,M}$ (since receive-side correlation is not affecting the row space of \mathbf{H}_k and $\widehat{\mathbf{H}}_k$; see Lemma 2). The performance loss can therefore be bounded using Lemma 3 and it only remains to characterize $\mathbb{E}\{\mathbf{H}_k \widehat{\mathbf{W}}_\ell^{\text{BD}} \widehat{\mathbf{W}}_\ell^{\text{BD},H} \mathbf{H}_k^H\}$ for $\ell \neq k$. From (28) we have

$$\mathbf{H}_k = \widehat{\mathbf{H}}_k + \mathbf{R}_{E,k}^{\frac{1}{2}} \tilde{\mathbf{E}}_k \quad (54)$$

where the second term is the estimation error, $\mathbf{R}_{E,k} = (\mathbf{R}_{R,k}^{-T} + \frac{\mathbf{T}_k^H \mathbf{T}_k}{\sigma^2})^{-1}$, and $\tilde{\mathbf{E}}_k$ has $\mathcal{CN}(0, 1)$ -entries. By using that $\widehat{\mathbf{H}}_k \widehat{\mathbf{W}}_\ell^{\text{BD}} = \mathbf{0}$ for $\ell \neq k$, we achieve

$$\mathbb{E}\{\mathbf{H}_k \widehat{\mathbf{W}}_\ell^{\text{BD}} \widehat{\mathbf{W}}_\ell^{\text{BD},H} \mathbf{H}_k^H\} = \mathbf{R}_{E,k}^{\frac{1}{2}} \mathbb{E}\{\tilde{\mathbf{E}}_k \widehat{\mathbf{W}}_\ell^{\text{BD}} \widehat{\mathbf{W}}_\ell^{\text{BD},H} \tilde{\mathbf{E}}_k^H\} \mathbf{R}_{E,k}^{\frac{1}{2}} \quad (55)$$

where $\mathbb{E}\{\tilde{\mathbf{E}}_k \widehat{\mathbf{W}}_\ell^{\text{BD}} \widehat{\mathbf{W}}_\ell^{\text{BD},H} \tilde{\mathbf{E}}_k^H\} = M \mathbf{I}_M$ since $\tilde{\mathbf{E}}_k$ is complex Gaussian and independent of $\widehat{\mathbf{W}}_\ell^{\text{BD}}$. Therefore, $\mathbb{E}\{\mathbf{H}_k \widehat{\mathbf{W}}_\ell^{\text{BD}} \widehat{\mathbf{W}}_\ell^{\text{BD},H} \mathbf{H}_k^H\} = M (\mathbf{R}_{R,k}^{-T} + \frac{\mathbf{T}_k^H \mathbf{T}_k}{\sigma^2})^{-1}$.

APPENDIX G PROOF OF LEMMA 1

Observe that $\mathbf{H} = \mathbf{R}_R^{1/2} \tilde{\mathbf{H}}$ has the same distribution as $\mathbf{H}\mathbf{U}$ for any unitary matrix \mathbf{U} . Thus, we can rotate \mathbf{h} arbitrarily without changing the statistics, meaning that $\frac{\mathbf{h}}{\|\mathbf{h}\|_2}$ must be isotropically distributed. Next, note that $\|\mathbf{h}\|_2^2 = \|\tilde{\mathbf{c}}^H \mathbf{H}\mathbf{U}\|_2^2 = \|\tilde{\mathbf{c}}^H \mathbf{H}\|_2^2$, thus unitary rotations will not affect the effective channel gain meaning that the direction and the channel gain are statistically independent. $\|\mathbf{h}\|_2^2$ is the dominating eigenvalue of the correlated complex Wishart matrix $\mathbf{H}\mathbf{H}^H \in \mathcal{W}_M(N, \mathbf{R}_R)$. The mean value expression in (32) can be achieved directly from [40, Theorem 3] or by using the moment generating function in [41] (which gives an equivalent expression that looks slightly different).

APPENDIX H
PROOF OF THEOREM 6

This theorem is proved in the same way as Theorem 5. The only notable difference is that we use the effective channel \mathbf{h}_k , which has a single effective receive antenna, instead of the original channel \mathbf{H}_k . The effective channel is zero-mean and has an average channel gain $\mathbb{E}\{\|\mathbf{h}_k\|_2^2\}$ given by (32). Thus, the effective channel and its channel estimate is related as $\mathbf{h}_k^H = \hat{\mathbf{h}}_k^H + (\frac{1}{\mathbb{E}\{\|\mathbf{h}_k\|_2^2\}} + \frac{\Psi}{\sigma^2})^{-1/2} \tilde{\mathbf{e}}_k^H$, where $\tilde{\mathbf{e}}_k \sim \mathcal{CN}(\mathbf{0}, \mathbf{I}_N)$.

REFERENCES

- [1] D. Gesbert, M. Kountouris, R. Heath, C.-B. Chae, and T. Sälzer, "Shifting the MIMO paradigm," *IEEE Signal Process. Mag.*, vol. 24, no. 5, pp. 36–46, 2007.
- [2] J. Hoydis, M. Kobayashi, and M. Debbah, "Green small-cell networks," *IEEE Veh. Technol. Mag.*, vol. 6, no. 1, pp. 37–43, 2011.
- [3] H. Weingarten, Y. Steinberg, and S. Shamai, "The capacity region of the Gaussian multiple-input multiple-output broadcast channel," *IEEE Trans. Inf. Theory*, vol. 52, no. 9, pp. 3936–3964, 2006.
- [4] R. Roy and B. Ottersten, "Spatial division multiple access wireless communication systems," US Patent 5515 378, 1996. [Online]. Available: http://www.patentlens.net/patentlens/patent/EP_0616742_B1/en/
- [5] Q. Spencer, A. Swindlehurst, and M. Haardt, "Zero-forcing methods for downlink spatial multiplexing in multiuser MIMO channels," *IEEE Trans. Signal Process.*, vol. 52, no. 2, pp. 461–471, 2004.
- [6] N. Ravindran and N. Jindal, "Limited feedback-based block diagonalization for the MIMO broadcast channel," *IEEE J. Sel. Areas Commun.*, vol. 26, no. 8, pp. 1473–1482, 2008.
- [7] N. Jindal, "Antenna combining for the MIMO downlink channel," *IEEE Trans. Wireless Commun.*, vol. 7, no. 10, pp. 3834–3844, 2008.
- [8] M. Trivellato, F. Boccardi, and H. Huang, "On transceiver design and channel quantization for downlink multiuser MIMO systems with limited feedback," *IEEE J. Sel. Areas Commun.*, vol. 26, no. 8, pp. 1494–1504, 2008.
- [9] A. Tölli and M. Juntti, "Scheduling for multiuser MIMO downlink with linear processing," in *Proc. IEEE PIMRC'05*, 2005, pp. 156–160.
- [10] F. Boccardi and H. Huang, "A near-optimum technique using linear precoding for the MIMO broadcast channel," in *Proc. IEEE ICASSP'07*, 2007.
- [11] R. Chen, Z. Shen, J. Andrews, and R. Heath, "Multimode transmission for multiuser MIMO systems with block diagonalization," *IEEE Trans. Signal Process.*, vol. 56, no. 7, pp. 3294–3302, 2008.
- [12] C. Guthy, W. Utschick, R. Hunger, and M. Joham, "Efficient weighted sum rate maximization with linear precoding," *IEEE Trans. Signal Process.*, vol. 58, no. 4, pp. 2284–2297, 2010.
- [13] A. Bayesteh and A. Khandani, "On the user selection for MIMO broadcast channels," *IEEE Trans. Inf. Theory*, vol. 54, no. 3, pp. 1086–1107, 2008.
- [14] W. Rhee, W. Yu, and J. Cioffi, "The optimality of beamforming in uplink multiuser wireless systems," *IEEE Trans. Wireless Commun.*, vol. 3, no. 1, pp. 86–96, 2004.
- [15] M. Dohler, R. Heath, A. Lozano, C. Papadias, and R. Valenzuela, "Is the PHY layer dead?" *IEEE Commun. Mag.*, vol. 49, no. 4, pp. 159–165, 2011.
- [16] D. Chizhik, J. Ling, P. Wolniansky, R. Valenzuela, N. Costa, and K. Huber, "Multiple-input-multiple-output measurements and modeling in Manhattan," *IEEE J. Sel. Areas Commun.*, vol. 21, no. 3, pp. 321–331, 2003.
- [17] K. Yu, M. Bengtsson, B. Ottersten, D. McNamara, P. Karlsson, and M. Beach, "Modeling of wide-band MIMO radio channels based on NLoS indoor measurements," *IEEE Trans. Veh. Technol.*, vol. 53, no. 3, pp. 655–665, 2004.
- [18] E. Björnson and B. Ottersten, "A framework for training-based estimation in arbitrarily correlated Rician MIMO channels with Rician disturbance," *IEEE Trans. Signal Process.*, vol. 58, no. 3, pp. 1807–1820, 2010.
- [19] G. Caire, N. Jindal, M. Kobayashi, and N. Ravindran, "Multiuser MIMO achievable rates with downlink training and channel state feedback," *IEEE Trans. Inf. Theory*, vol. 56, no. 6, pp. 2845–2866, 2010.
- [20] Z.-Q. Luo and S. Zhang, "Dynamic spectrum management: Complexity and duality," *IEEE J. Sel. Topics Signal Process.*, vol. 2, no. 1, pp. 57–73, 2008.
- [21] Q. Shi, M. Razaviyayn, Z.-Q. Luo, and C. He, "An iteratively weighted MMSE approach to distributed sum-utility maximization for a MIMO interfering broadcast channel," *IEEE Trans. Signal Process.*, vol. 59, no. 9, pp. 4331–4340, 2011.
- [22] J. Lee and N. Jindal, "High SNR analysis for MIMO broadcast channels: Dirty paper coding vs. linear precoding," *IEEE Trans. Inf. Theory*, vol. 53, no. 12, pp. 4787–4792, 2007.
- [23] T. Yoo and A. Goldsmith, "On the optimality of multi-antenna broadcast scheduling using zero-forcing beamforming," *IEEE J. Sel. Areas Commun.*, vol. 24, no. 3, pp. 528–541, 2006.
- [24] S. Loyka, "Channel capacity of MIMO architecture using the exponential correlation matrix," *IEEE Commun. Lett.*, vol. 5, no. 9, pp. 369–371, 2001.
- [25] E. Björnson, D. Hammarwall, and B. Ottersten, "Exploiting quantized channel norm feedback through conditional statistics in arbitrarily correlated MIMO systems," *IEEE Trans. Signal Process.*, vol. 57, no. 10, pp. 4027–4041, 2009.
- [26] Z. Shen, R. Chen, J. Andrews, R. Heath, and B. Evans, "Low complexity user selection algorithms for multiuser MIMO systems with block diagonalization," *IEEE Trans. Signal Process.*, vol. 54, no. 9, pp. 3658–3663, 2006.
- [27] E. Björnson, M. Bengtsson, and B. Ottersten, "Receive combining vs. multistream multiplexing in multiuser MIMO systems," in *Proc. IEEE Swe-CTW'11*, 2011, pp. 109–114.
- [28] D. Love, R. Heath, and T. Strohmer, "Grassmannian beamforming for multiple-input multiple-output wireless systems," *IEEE Trans. Inf. Theory*, vol. 49, no. 10, pp. 2735–2747, 2003.
- [29] W. Dai, Y. Liu, and B. Rider, "Quantization bounds on Grassmann manifolds and applications to MIMO communications," *IEEE Trans. Inf. Theory*, vol. 54, no. 3, pp. 1108–1123, 2008.
- [30] V. Raghavan, R. Heath, and A. Sayeed, "Systematic codebook designs for quantized beamforming in correlated MIMO channels," *IEEE J. Sel. Areas Commun.*, vol. 25, no. 7, pp. 1298–1310, 2007.
- [31] D. Love, R. Heath, V. Lau, D. Gesbert, B. Rao, and M. Andrews, "An overview of limited feedback in wireless communication systems," *IEEE J. Sel. Areas Commun.*, vol. 26, no. 8, pp. 1341–1365, 2008.
- [32] S. Zhou and B. Li, "BER criterion and codebook construction for finite-rate precoded spatial multiplexing with linear receivers," *IEEE Trans. Signal Process.*, vol. 54, no. 5, pp. 1653–1665, 2006.
- [33] W. Santipach and M. Honig, "Asymptotic capacity of beamforming with limited feedback," in *Proc. IEEE ISIT'04*, 2004, p. 290.
- [34] C. Au-Yeung and D. Love, "On the performance of random vector quantization limited feedback beamforming in a MISO system," *IEEE Trans. Wireless Commun.*, vol. 6, no. 2, pp. 458–462, 2007.
- [35] M. Kountouris, R. de Francisco, D. Gesbert, D. Slock, and T. Sälzer, "Multiuser diversity - multiplexing tradeoff in MIMO broadcast channels with limited feedback," in *Proc. ACSSC'06*, 2006, pp. 364–368.
- [36] N. Ravindran and N. Jindal, "Multi-user diversity vs. accurate channel feedback for MIMO broadcast channels," in *Proc. IEEE ICC'08*, 2008, pp. 3684–3688.
- [37] N. Jindal, "MIMO broadcast channels with finite-rate feedback," *IEEE Trans. Inf. Theory*, vol. 52, no. 11, pp. 5045–5060, 2006.
- [38] T. Yoo, N. Jindal, and A. Goldsmith, "Multi-antenna downlink channels with limited feedback and user selection," *IEEE J. Sel. Areas Commun.*, vol. 25, no. 7, pp. 1478–1491, 2007.
- [39] D. Hammarwall, M. Bengtsson, and B. Ottersten, "Acquiring partial CSI for spatially selective transmission by instantaneous channel norm feedback," *IEEE Trans. Signal Process.*, vol. 56, no. 3, pp. 1188–1204, 2008.
- [40] E. Björnson and B. Ottersten, "Post-user-selection quantization and estimation of correlated Frobenius and spectral channel norms," in *Proc. IEEE PIMRC'08*, 2008.
- [41] M. McKay, I. Collings, and P. Smith, "Capacity and SER analysis of MIMO beamforming with MRC," in *Proc. IEEE ICC'06*, 2006.